JCI The Journal of Clinical Investigation

Tuberous sclerosis complex–mediated mTORC1 overactivation promotes age-related hearing loss

Xiaolong Fu, … , Haibo Wang, Jiangang Gao

J Clin Invest. 2018;128(11):4938-4955. https://doi.org/10.1172/JCI98058.

Research Article Aging Neuroscience

The underlying molecular mechanisms of age-related hearing loss (ARHL) in humans and many strains of mice have not been fully characterized. This common age-related disorder is assumed to be closely associated with oxidative stress. Here, we demonstrate that mTORC1 signaling is highly and specifically activated in the cochlear neurosensory epithelium (NSE) in aging mice, and rapamycin injection prevents ARHL. To further examine the specific role of mTORC1 signaling in ARHL, we generated murine models with NSE-specific deletions of *Raptor* or *Tsc1*, regulators of mTORC1 signaling. *Raptor-cKO* mice developed hearing loss considerably more slowly than WT littermates. Conversely,*Tsc1* loss led to the early-onset death of cochlear hair cells and consequently accelerated hearing loss. *Tsc1-cKO* cochleae showed features of oxidative stress and impaired antioxidant defenses. Treatment with rapamycin and the antioxidant *N*-acetylcysteine rescued *Tsc1-cKO* hair cells from injury in vivo. In addition, we identified the peroxisome as the initial signaling organelle involved in the regulation of mTORC1 signaling in cochlear hair cells. In summary, our findings identify overactive mTORC1 signaling as one of the critical causes of ARHL and suggest that reduction of mTORC1 activity in cochlear hair cells may be a potential strategy to prevent ARHL.

Find the latest version:

https://jci.me/98058/pdf

Tuberous sclerosis complex–mediated mTORC1 overactivation promotes age-related hearing loss

Xiaolong Fu,[1] Xiaoyang Sun,[1] Linqing Zhang,[1] Yecheng Jin,[1] Renjie Chai,[2] Lili Yang,[1] Aizhen Zhang,[1,3] Xiangguo Liu,[1] Xiaochun Bai,[4] Jianfeng Li,[3] Haibo Wang,[3] and Jiangang Gao[1]

[1]School of Life Science and Key Laboratory of the Ministry of Education for Experimental Teratology, Shandong University, Jinan, China. [2]Key Laboratory for Development Genes and Human Disease, Southeast University, Nanjing, China. [3]Department of Otolaryngology–Head and Neck Surgery, Provincial Hospital Affiliated to Shandong University, Jinan, China. [4]State Key Laboratory of Organ Failure Research, Department of Cell Biology, School of Basic Medical Sciences, Southern Medical University, Guangzhou, China.

The underlying molecular mechanisms of age-related hearing loss (ARHL) in humans and many strains of mice have not been fully characterized. This common age-related disorder is assumed to be closely associated with oxidative stress. Here, we demonstrate that mTORC1 signaling is highly and specifically activated in the cochlear neurosensory epithelium (NSE) in aging mice, and rapamycin injection prevents ARHL. To further examine the specific role of mTORC1 signaling in ARHL, we generated murine models with NSE-specific deletions of *Raptor* or *Tsc1*, regulators of mTORC1 signaling. *Raptor-cKO* mice developed hearing loss considerably more slowly than WT littermates. Conversely, *Tsc1* loss led to the early-onset death of cochlear hair cells and consequently accelerated hearing loss. *Tsc1-cKO* cochleae showed features of oxidative stress and impaired antioxidant defenses. Treatment with rapamycin and the antioxidant *N*-acetylcysteine rescued *Tsc1-cKO* hair cells from injury in vivo. In addition, we identified the peroxisome as the initial signaling organelle involved in the regulation of mTORC1 signaling in cochlear hair cells. In summary, our findings identify overactive mTORC1 signaling as one of the critical causes of ARHL and suggest that reduction of mTORC1 activity in cochlear hair cells may be a potential strategy to prevent ARHL.

Introduction

Age-related hearing loss (ARHL), also known as presbycusis, is one of the most common sensory disorders in elderly individuals. This condition occurs in 25%–40% of people aged 65 years or older, and its prevalence increases with age, ranging from 40% to 66% in people older than 75 years (1, 2). ARHL is not usually apparent at the initial onset and progresses slowly, starting with the loss of high-frequency detection. Most people are not conscious of a hearing problem until medium-frequency dysfunction appears, which may affect daily communication (3).

ARHL is characterized by the degeneration of auditory function and is a complex, multifactorial disorder involving environmental, genetic, health, and nutritional factors (4, 5). The primary pathology of ARHL includes hair cell loss and the loss of spiral ganglion neurons (SGNs) as well as changes in central auditory pathways (6, 7). Despite intense efforts to clarify the pathogenesis of ARHL, the detailed underlying mechanisms remain largely unknown. Research to date suggests that oxidative stress plays a major role in the pathophysiology of ARHL, and attention has centered on the contribution of reactive oxygen species (ROS) to age-related hearing cellular degeneration. ROS arise from multiple sources and are generated as radicals or proradicals by, among others, NADPH oxidase, mitochondrial, peroxisomal, or microsomal pathways (8). Findings from numerous studies suggest that oxidative damage in the cochlea reflects an age-related decline in antioxidant defenses and/or an age-related increase in ROS levels and plays a crucial role in the development of ARHL (9–11). Moreover, targeting oxidative stress via pharmacological or genetic interventions prevents or slows ARHL (12–14). However, the effects of antioxidant supplementation on the prevention of ARHL are currently controversial and inconclusive. Additionally, the short duration of action of these chemical inhibitors or antioxidants limits their clinical utility in the treatment of ARHL. Therefore, the development of antioxidant therapy for ARHL requires a detailed understanding of underlying oxidative stress mechanisms.

Mammalian target of rapamycin (mTOR) is a serine/threonine kinase that coordinates numerous cellular processes. It assembles into 2 multiprotein complexes: the rapamycin-sensitive mTOR complex 1 (mTORC1) and the rapamycin-insensitive mTORC2 (15). The mTORC1 complex, consisting of mTOR, Raptor, and mLST8, is thought to control autonomous cell growth in response to nutrient availability and growth factors (16–18). The tuberous sclerosis complex (TSC), which is composed of Tsc1 and Tsc2, is involved in the negative regulation of mTORC1 activity (19). Disruption of this complex through the loss of either Tsc1 or Tsc2 results in constitutive activation of mTORC1 that is largely independent of cellular growth conditions. Many age-related diseases are related to mTORC1 signaling (20, 21). For example, mTORC1 is hyperactivated in platelets and megakaryocytes in aged mice (22). Over the past decade, a handful of studies have estimated that inhibition of the mTORC1 pathway confers protection against a growing list of age-related pathologies (23, 24). Accumulating

Conflict of interest: The authors have declared that no conflict of interest exists.
Submitted: October 16, 2017; **Accepted:** August 8, 2018.
Reference information: *J Clin Invest*. 2018;128(11):4938–4955.
https://doi.org/10.1172/JCI98058.

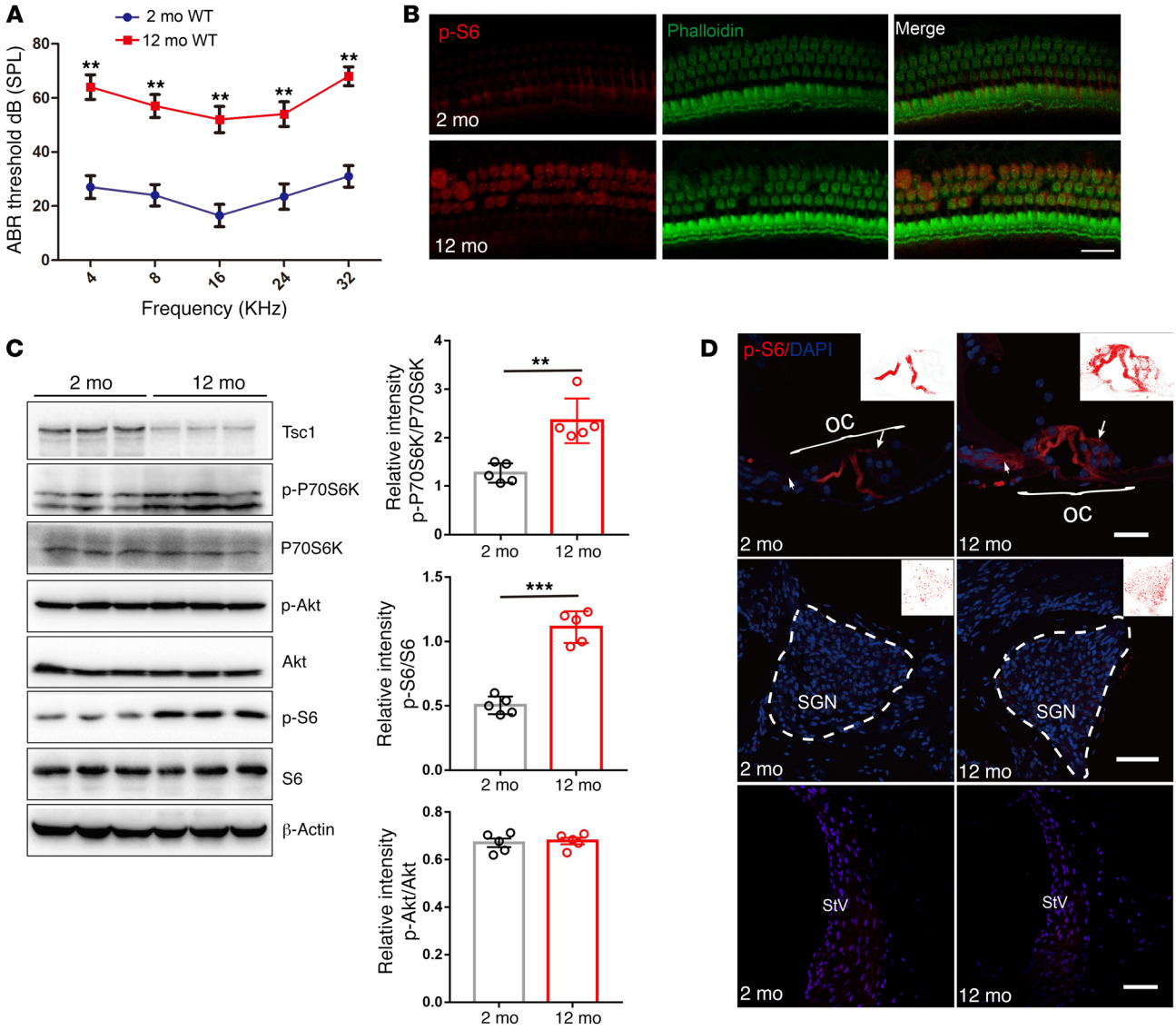

Figure 1. mTORC1 signaling is activated in the NSE of aging cochlea in C57BL/6J mice. (**A**) ABR hearing thresholds were increased in 12-month-old WT mice compared with 2-month-old WT mice. $n = 10$. (**B**) Representative images of immunolabeled p-S6 (red) in OHCs with phalloidin staining (green) in 12-month-old WT mice and 2-month-old WT mice. $n = 3$. Scale bar: 10 μm. (**C**) Western blot analysis of sensory epithelium shows increased p-P70S6K and p-S6 (235/236) levels and decreased Tsc1 levels, without any alterations in p-Akt (S473) levels, in 12-month-old WT mice compared with 2-month-old WT mice; p-P70S6K, p-S6 (235/236), and p-Akt (S473) levels are quantified on the right side. Protein lysates were obtained from sensory epithelial tissues from cochleae. β-Actin served as the sample loading control; $n = 5$. See complete unedited blots in the supplemental material. (**D**) p-S6 immunolabeling (red) was stronger in middle hair cells (arrows) and Deiters cells in the organ of Corti (OC) in 12-month-old WT mice than in 2-month-old WT mice; however, no significant changes were detected in the pillar cells, the SGN, and the stria vascularis (StV). $n = 3$. Scale bars: 20 μm. Data represent the mean ± SEM. $^{**}P < 0.01$, $^{***}P < 0.001$, by 2-tailed Student's t test.

evidence has suggested that mTORC1 acts downstream of caloric restriction (CR), and CR reduces mTORC1 activity in several mammalian tissues (25–27). On one hand, mTORC1 signaling is thought to play a role in mediating longevity and health benefits as a result of CR (20). On the other hand, CR is also known to extend lifespan in yeast, worms, fruit flies, spiders, birds, and monkeys and delays the progression of a variety of age-associated diseases such as cancer, diabetes, cataracts, and ARHL in mammals (28, 29). Thus, numerous studies describing the complex relationship between mTORC1 and age-associated diseases collectively suggest that mTORC1 may play a role in ARHL.

In the current study, we observed a significant increase in mTORC1 activity in the aging cochlear neurosensory epithelium (NSE). Inhibition of mTORC1 with rapamycin or a genetic reduction in mTORC1 activity in the NSE via the deletion of *Raptor*, an essential component of mTORC1, attenuated ARHL in C57BL/6J mice. Furthermore, using an NSE-specific conditional-*Tsc1*-knockout mouse model, we showed that sustained mTORC1 activation disrupted the redox balance in NSE, thus causing early-onset death of cochlear hair cells and progressive hearing loss. These results collectively indicate that overactive mTORC1 signaling in NSE is a critical factor in the development

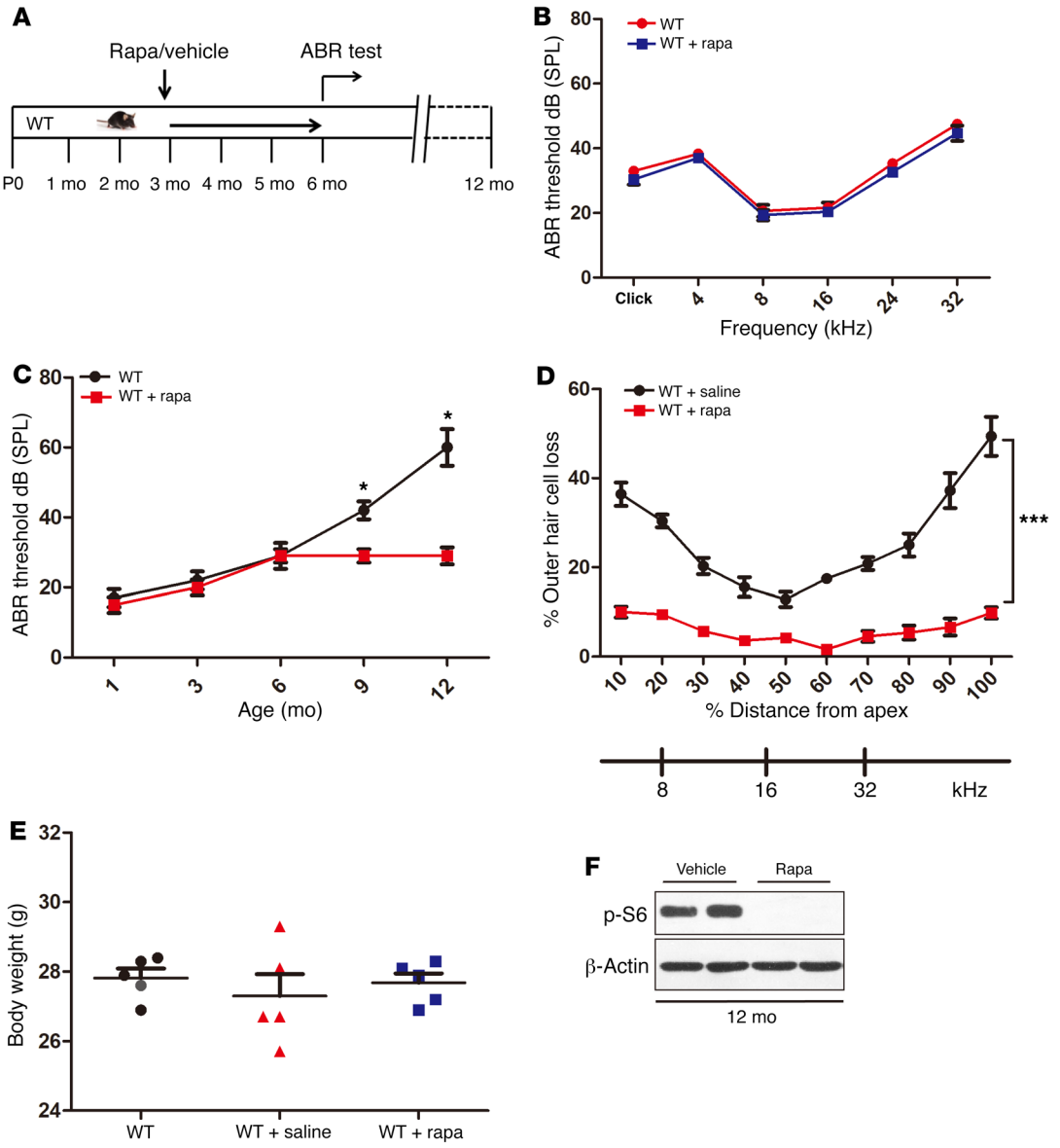

Figure 2. Rapamycin protects aged mice against ARHL. (**A**) Schematic of rapamycin treatment to examine its effects on ARHL in C57BL/6J mice. (**B**) ABR thresholds of the rapamycin-treated mice (1 mg/kg i.p. every other day from 3 months of age to 6 months) and the controls at the age of 6 months (n = 5). Broadband click and 4-, 8-, 16-, 24-, and 32-kHz stimuli were used in the ABR measurement. No significant differences were observed between the 2 groups. (**C**) ABR thresholds of the rapamycin-treated groups and controls to click stimuli at different ages. n = 6. (**D**) Hair cell loss as a percentage for both rapamycin-treated groups and controls; n = 5. (**E**) Comparison of the weights of control and rapamycin-treated C57BL/6J mice at 6 months of age; n = 5. No obvious differences in body weights were found between the rapamycin-treated groups and controls. (**F**) Lysates obtained from the whole cochleae of rapamycin-treated groups and controls at 12 months of age were analyzed by immunoblotting using an antibody targeting p-S6; n = 5. Data represent the mean ± SEM. $^*P < 0.05$, $^{***}P < 0.001$, by 2-tailed Student's t test.

of ARHL and suggest that targeting the mTORC1 pathway may shed new light on preventing ARHL.

Results

Tsc/mTORC1 signaling is activated in the NSE in aged C57BL/6J mice. The C57BL/6J mouse strain is the most widely used animal model for the study of ARHL, because it carries the recessive early-onset hearing loss susceptibility allele (*Cdh23*^{753A}) (30). We confirmed that the mean auditory brainstem response (ABR) hearing thresholds were significantly elevated at all frequencies (4, 8, 16, 24, and 32 kHz) in 12-month-old C57BL/6J mice compared with those in 2-month-old C57BL/6J mice (Figure 1A), indicating that the older mice displayed ARHL. Hair cell degeneration and spiral ganglion cell (SGC) degeneration are hallmarks of ARHL. Consistent with the ABR results, basal regions of the cochleae exhibited hair cell and SGC losses in 12-month-old WT mice (data not shown).

To investigate whether mTORC1 signaling is involved in the development of ARHL, we first examined the levels of S6 phosphorylation at 235/236 (p-S6), a downstream target of mTORC1 that is frequently used as an in vivo indicator of mTORC1 activ-

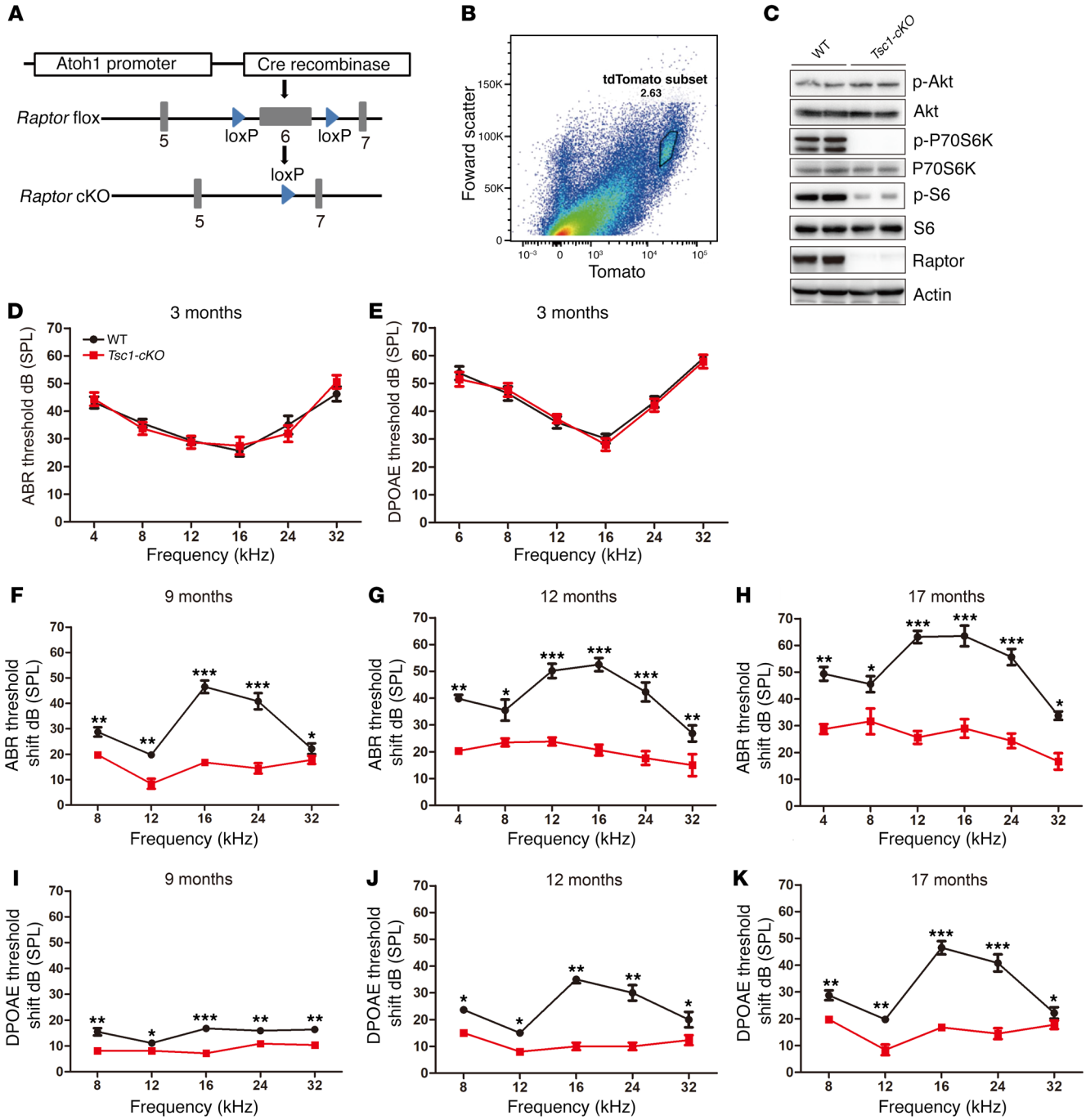

Figure 3. Deletion of mTORC1 in the NSE protects mice against ARHL. (**A**) Mice containing a floxed *Raptor* allele were crossed with transgenic mice expressing Cre under the control of the *Atoh1* promoter. The resultant Cre-mediated deletion of *Raptor* exon 6 leads to a frameshift mutation that produces a nonfunctional protein. (**B**) The tdTomato-positive cells were isolated using FACS. tdTomato-positive hair cells (2.63%) were encircled by the solid line. (**C**) tdTomato-positive cells were sorted out for Western blot. Western blot analysis of the tdTomato-positive cells revealed a dramatic decrease in Raptor expression and inactivation of mTORC1 (decreased expression of p-S6 and p-P70S6K) in *Raptor-cKO/tdTomato* mice. The 2 columns with the same label indicate the same sample loaded onto a second well; $n \geq 3$ for each group. (**D**–**K**) Reduced age-related threshold shifts in *Raptor-cKO* mice, as measured by either ABR (**D** and **F**–**H**) or DPOAE assessments (**E** and **I**–**K**). Threshold shifts were compared between *Raptor-cKO* ($n \geq 6$) and WT ($n \geq 4$) mice at the same time point (9, 12, and 17 months, respectively). The group sizes were as follows: 3 months: $n = 4$ for control, $n = 8$ for *Raptor-cKO*; 9 months: $n = 5$ for control, $n = 8$ for *Raptor-cKO*; 12 months: $n = 6$ for each group; 17 months: $n = 6$ for control, $n = 8$ for *Raptor-cKO*. Data represent the mean ± SEM. $^*P < 0.5$, $^{**}P < 0.01$, $^{***}P < 0.001$, by 2-tailed Student's *t* test.

ity in the cochlear hair cells of C57BL/6J mice. Immunolabeling for p-S6 in middle-turn outer hair cells (OHCs) was enhanced in 12-month-old mice compared with that in 2-month-old mice (Figure 1B). Western blot analysis using sensory epithelium tissues also demonstrated increased p-S6 (235/236) and p-P70S6K, another downstream target of mTORC1 (Figure 1C). In contrast, p-Akt (Ser473), the site regulated by mTORC2 activity, was stable with age, suggesting specific mTORC1 activation in NSE

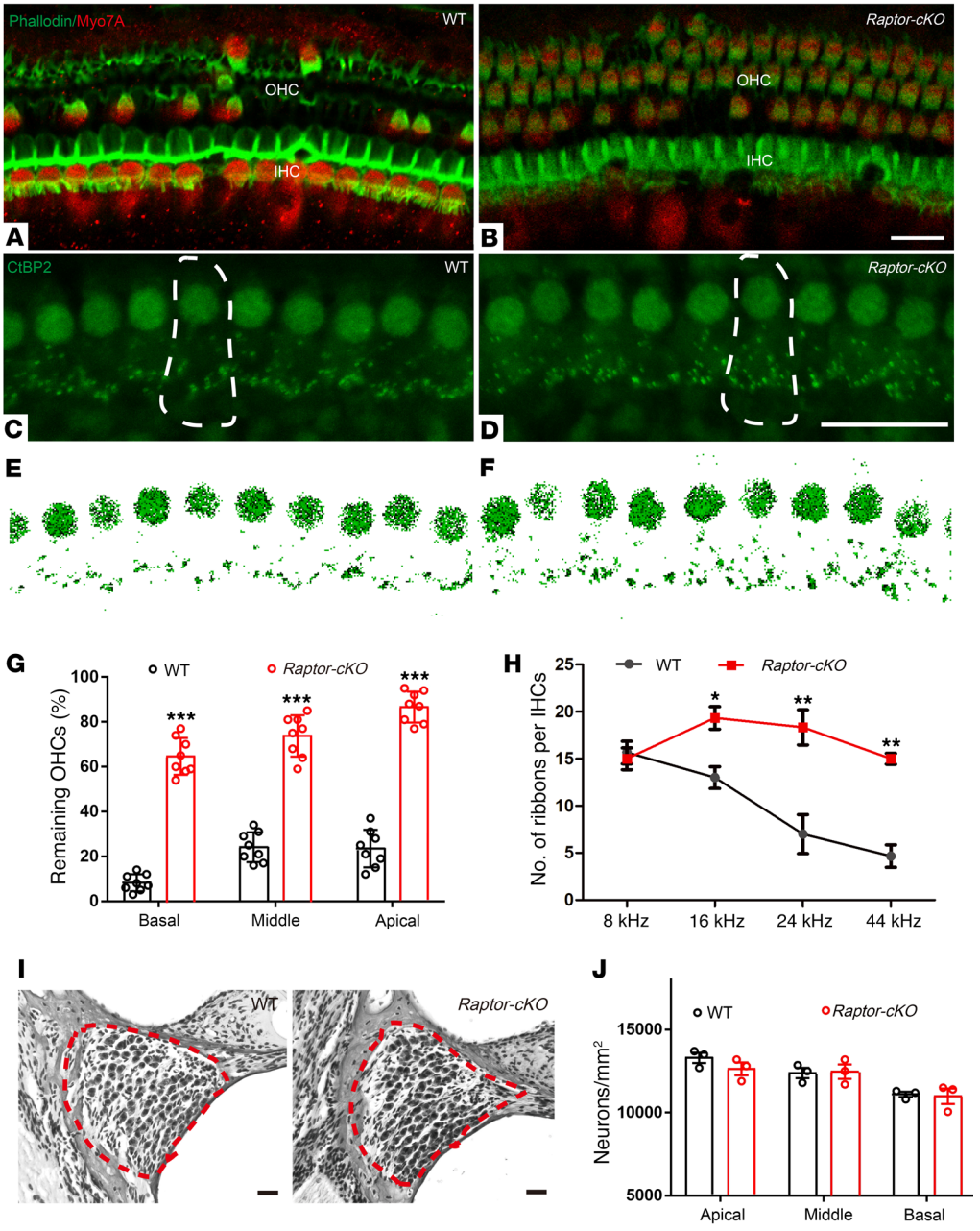

Figure 4. More hair cells survived and more presynaptic ribbons were retained in *Raptor-cKO* mice than in WT mice. (**A** and **B**) Confocal images of surface views of the organs of Corti from the 8-kHz region stained with Myo7A (which labels inner and outer hair cells, red) and phalloidin (which labels filamentous actin, green) in 17-month-old cochleae from WT and *Raptor-cKO* mice. $n = 4$. (**C**–**F**) Ribbons are stained with antibodies to CtBP2 (green) in 17-month-old cochleae from WT ($n = 6$) and *Raptor-cKO* mice ($n = 7$). A single IHC is outlined with dotted lines. (**G**) Hair cell counts from 17-month-old animals of both genotypes revealed that more hair cells survived in all 3 turns of the cochlea from *Raptor-cKO* mice ($n = 8$) compared with controls ($n = 8$). (**H**) More ribbon synapses remained in the *Raptor-cKO* mice ($n = 8$) than in the WT mice ($n = 6$) when measured at 17 months old. (**I** and **J**) Representative images and graphs illustrating the average numbers of SGNs in the cochleae of WT and *Raptor-cKO* mice. Similar ganglion cell survival patterns were observed in 17-month-old *Raptor-cKO* and WT middle turn sections by H&E staining. SGNs are surrounded by a dashed red line. SGN densities were counted and quantified in the cochleae of WT and *Raptor-cKO* mice; $n = 3$. Data represent the mean ± SEM. $^*P < 0.05$, $^{**}P < 0.01$, $^{***}P < 0.001$, by 1-way ANOVA with Holm-Šidák multiple-comparisons test. Scale bars: 20 μm.

(Figure 1C). We also found specific mTORC1 activation in DBA and BALB/c mouse lines, which also have ARHL (Supplemental Figure 1, A and B; supplemental material available online with this article; https://doi.org/10.1172/JCI98058DS1). To evaluate the location of the increased p-S6 (235/236) in key regions of the cochlea, SGNs, the lateral wall, and the organ of Corti, p-S6 (235/236) was immunolabeled in cochlear paraffin-embedded sections. In 2-month-old mice, p-S6 was rarely observed in hair cells (inner hair cells [IHCs] and OHCs) and Deiters cells, but strong expression was observed in the outer and inner pillar cells (Figure 1D). p-S6 expression levels were enhanced in hair cells and Deiters cells in aged mice; however, no obvious changes were detected in the pillar cells, the SGNs, and the stria vascularis (Figure 1D). Collectively, these results demonstrated that mTORC1 activity in NSE increased with age in mice, raising the possibility that dysregulated mTORC1 signaling plays a role in the development of ARHL.

Rapamycin protects aged mice against ARHL. Next, to determine whether activated mTORC1 signaling plays a role in the occurrence of ARHL, we examined the effects of the administration of rapamycin (a widely used mTORC1-specific inhibitor; ref. 31) in young and aged C57BL/6J mice (Figure 2A). Rapamycin was administered i.p. to mice every other day. Interestingly, the mean ABR thresholds of 6-month-old WT mice with or without 3 months of rapamycin treatment showed no significant differences, implying that rapamycin does not affect hearing in young mice (Figure 2B). However, rapamycin protected against ARHL in aged (12-month-old) mice, as shown by the significant observed decreases in the ABR threshold and hair cell loss in treated animals relative to age-matched controls (Figure 2, C

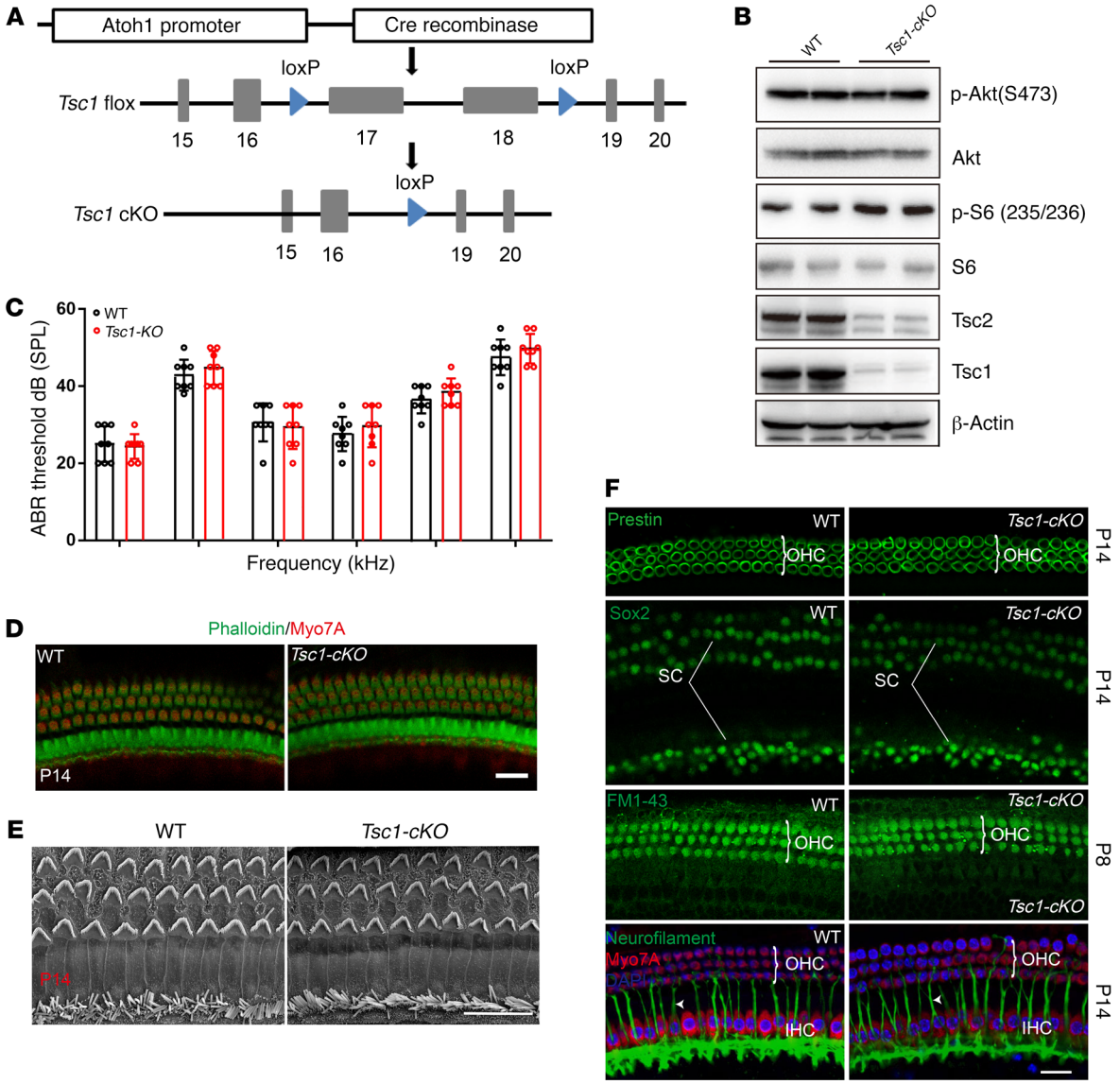

Figure 5. *Tsc1-cKO* mice show normal hearing development. (**A**) Regulatory elements of the *Atoh1* promoter drive the expression of *Cre* in NSE. (**B**) Immunoblotting confirmed that Tsc1 is absent from *Tsc1-cKO* mice. Tsc2 protein levels were also diminished, because Tsc1 stabilizes Tsc2. *Tsc1-cKO* mice displayed elevated mTORC1 activity, as demonstrated by the increased expression of p-S6 (235/236). However, phosphorylation of Akt at Ser473 was not affected by active mTORC1 expression. $n = 5$. (**C**) ABR thresholds of *Tsc1-cKO* ($n = 5$) and WT mice ($n = 5$) (both at 14 days after birth) to click stimuli and to 4-, 8-, 16-, 24-, and 32-kHz stimuli were measured. No significant differences were observed between genotypes. (**D**) Confocal images showed no differences in hair cells from the 8-kHz region between *Tsc1-cKO* mice ($n = 3$) and controls ($n = 3$) at P14. Green, phalloidin; red, Myo7A. (**E**) Low-magnification SEM images of cochlear stereociliary bundles of *Tsc1-cKO* and WT mice at P14; $n = 3$. (**F**) There were no significant differences in the distribution of key proteins, including prestin for OHCs, Sox2 for supporting cells, and neurofilament (arrowheads) for nerve fibers. FM1-43 uptake by auditory hair cells at P8 confirmed their normal function. $n = 3$. Scale bars: 20 μm. Data represent the mean ± SEM.

and D). In addition, there were no obvious differences in gross morphology and body weight between the rapamycin-treated groups and controls (Figure 2E). Western blot results revealed that all p-S6 (235/236) detected in the cochlea was eliminated by rapamycin treatment (Figure 2F). Rapamycin injection can also make DBA and BALB/c mice resistant to ARHL (Supplemental Figure 2, A and B). Collectively, these findings confirmed mTORC1 activation as a pathogenic factor driving the development of ARHL and demonstrated that the inhibition of mTORC1 by rapamycin prevented ARHL.

Inactivation of mTORC1 signaling in NSE alleviates ARHL. Whole-body rapamycin treatment affects not only the NSE but also other cochlear cell types, such as SGNs and the stria vascularis. Therefore, although inhibition of mTORC1 signaling by rapamycin alleviates ARHL, it is not clear whether inhibition of mTORC1 signaling in NSE alone is sufficient to prevent ARHL. To answer this question, we generated mice exhibiting conditional ablation (cKO) of the mTORC1-specific component *Raptor* in the NSE using a *Cre* recombinase expression cassette (Figure 3A). An *Atoh1-Cre* mouse line was selected in this study because it report-

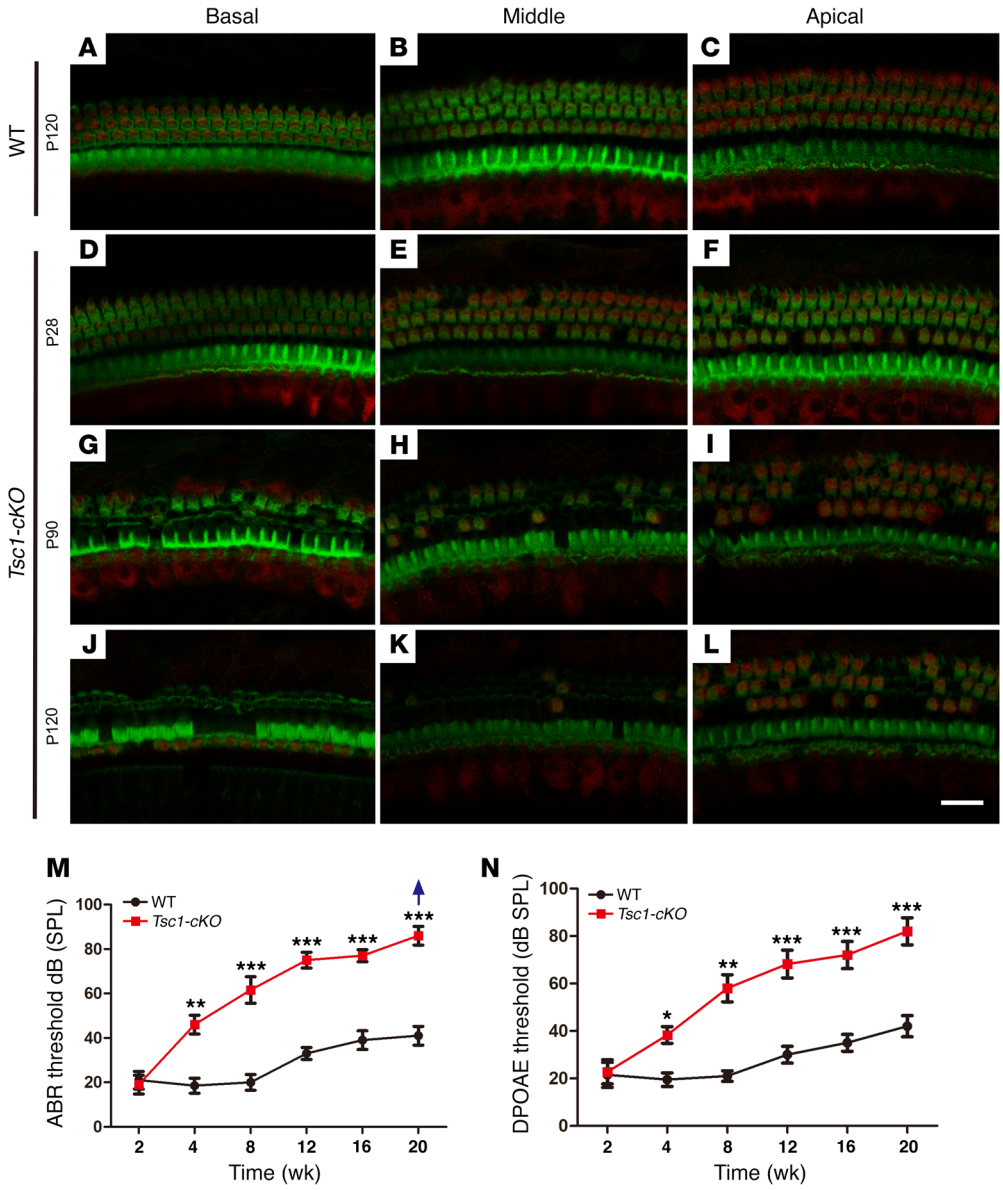

Figure 6. *Tsc1-cKO* mice undergo hair cell degeneration and gradual hearing loss from the fourth week of life. Confocal images of cochlear whole mounts labeled with a Myo7A antibody (red) and counterstained with phalloidin to label filamentous actin (green) are shown. (**A**–**C**) Representative images from the basal, middle, and apical turns of the organ of Corti in WT mice at P120. (**D**–**L**) Representative images of the organ of Corti from 3 turns of the cochleae in *Tsc1-cKO* mice at P28 (**D**–**F**), P90 (**G**–**I**), and P120 (**J**–**L**). OHCs began to degenerate by P28. Severe degeneration was evident at P90. By P120, only a few OHCs and partial IHCs remained in the middle and apical turns of the cochleae. n = 5 for each group. (**M** and **N**) Graphs illustrate age-dependent threshold changes in WT and *Tsc1-cKO* mice. Age-related click ABR thresholds (**M**) and age-related DPOAE thresholds (**N**) in WT and *Tsc1-cKO* mice showed progressive hearing loss. The group sizes were as follows: 2 and 4 weeks: n = 15 for each group; 8, 12, 16, and 20 weeks: n = 5 for each group. The arrow indicates that even at the highest SPL test level (90 dB SPL), several *Tsc1-cKO* mice showed no response. Data are shown as the mean ± SD. $^{*}P < 0.05$, $^{**}P < 0.01$, $^{***}P < 0.001$, by 2-tailed Student's t test. Scale bar: 20 μm.

edly specifically and efficiently deletes loxP-floxed regions in nearly all inner ear hair cells as well as in supporting cells of all types (32). To confirm that recombination had occurred in the NSE, we generated *Atoh1-Cre/Raptor*$^{fl/fl}$*/Rosa26-tdTomato* mice and isolated tdTomato-positive cells using flow cytometry (Figure 3B). tdTomato-positive cells were sorted out for Western blot. Western blot analysis revealed that the expression of Raptor in NSE was disrupted in *Atoh1-Cre/Raptor*$^{fl/fl}$*/Rosa26-tdTomato* mice. The inactivation of mTORC1 signaling was confirmed by reduced levels of p-S6 (235/236) and p-P70S6K relative to controls (Figure 3C). In contrast, the expression levels of p-Akt (Ser473), the site regulated by mTORC2, were stable in *Raptor-cKO* mouse NSE (Figure 3C). Therefore, *Raptor-cKO* mice demonstrate NSE-specific inactivation of the mTORC1 signaling pathway.

The gross morphology of *Raptor-cKO* mice was similar to that of their control littermates, indicating no markedly obvious developmental defects. Based on H&E staining of cochlear sections, *Raptor-cKO* mice also exhibited no visible structural alterations in the inner ear compared with WT mice (data not shown). Next, to detect whether inactivation of the mTORC1 signaling pathway prevents ARHL, we carried out electrophysiological tests of cochlear function at different ages. At 3 months, the mean ABR thresholds in *Raptor-cKO* mice were virtually identical to those in the controls (Figure 3D). There was a dramatic elevation (>40 dB) in mean ABR thresholds characteristic of ARHL from 3 months to 17 months of age in the WT mice. However, the mean ABR threshold elevation (~15 dB) from 3 months to 17 months of age in *Raptor-cKO* mice was not as obvious as that in WT mice. Compared with 3 months, the mean ABR threshold shifts at all frequencies in *Raptor-cKO* mice were significantly smaller than that in WT mice at 9, 12, or 17 months of age (Figure 3, F–H). Distortion product otoacoustic emission (DPOAE) was used to detect a low-level sound generated by the active mechanism of OHCs emitted to the ear canal. At 3 months, similar DPOAEs were observed between *Raptor-cKO* mice and controls (Figure 3E). In contrast, at later stages, the DPOAE threshold shifts in *Raptor-cKO* mice were significantly

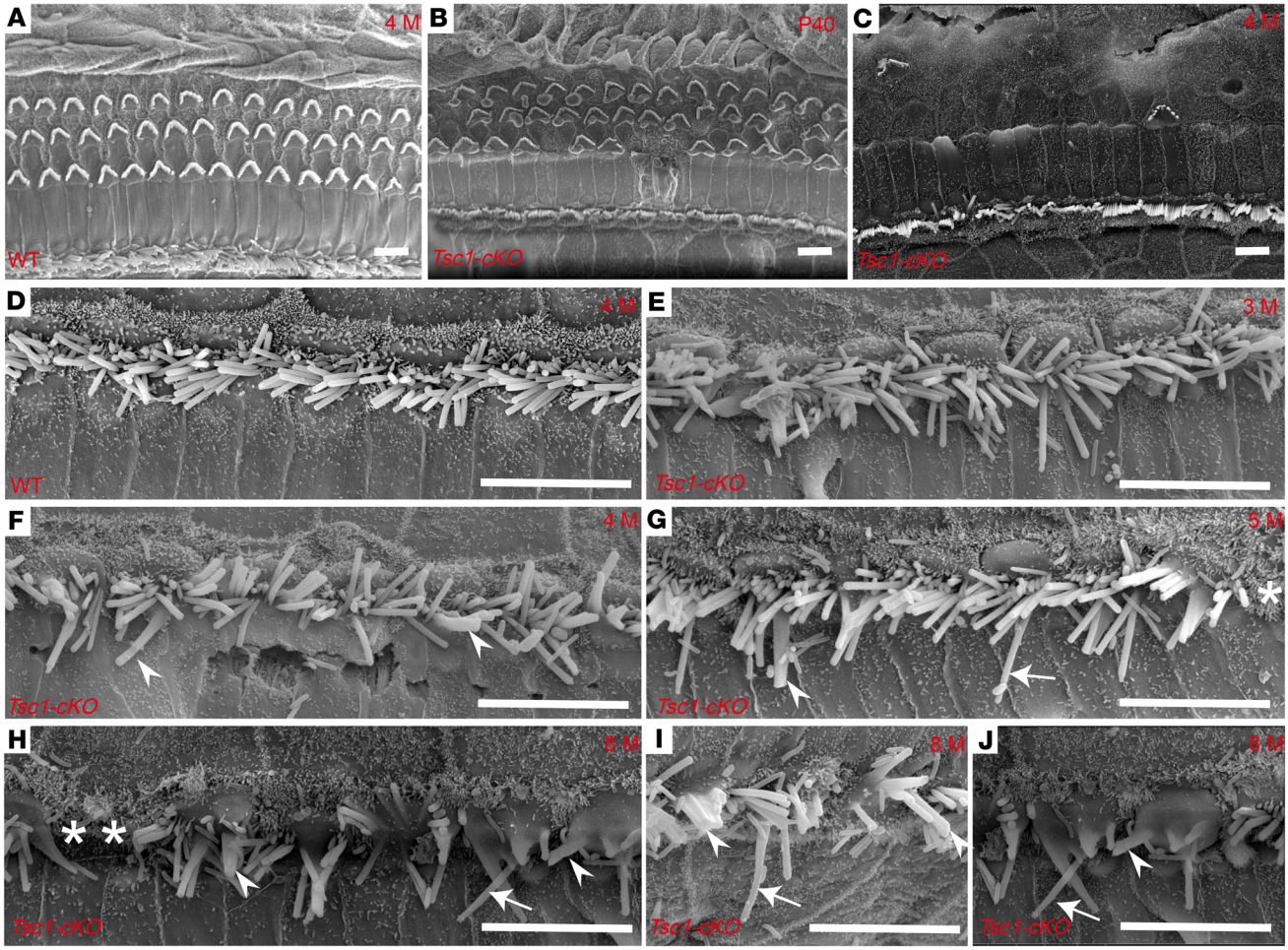

Figure 7. Degeneration of cochlear stereocilia in *Tsc1-cKO* mice. SEM images of the organ of Corti at the middle turn obtained from *Tsc1-cKO* (**B**, **C**, and **E**–**J**) and WT (**A** and **D**) mice. (**A**) Both OHCs and IHCs were regular and aligned normally in WT mice at 4 months. (**B**) OHCs were partially lost in *Tsc1-cKO* mice at P40. (**C**) In *Tsc1-cKO* mice at 4 months, OHCs mostly disappeared, whereas IHCs appeared to be normally regulated along the basilar membrane of the cochlea. (**D**) The normal morphology of IHCs in the middle turns of the cochlea in WT mice at 4 months. (**E**) Fused stereocilia (arrowheads) were first observed at 3 months in the middle turn of the cochlea in *Tsc1-cKO* mice. (**F**–**J**) Fused stereocilia (arrowheads) increased in number from 4 months (**F**) to 8 months (**H**). Lost IHCs (asterisks) began to appear at 5 months (**G**) in the middle turn of the cochlea in *Tsc1-cKO* mice. The middle turn of the cochlea in *Tsc1-cKO* mice at 8 months retained several IHCs (**H**–**J**), which frequently demonstrate long stereocilia (arrows) and fused stereocilia (arrowheads). n = 5 for each group. Scale bars: 10 μm.

smaller than those in control mice. However, the differences were smaller than those seen in corresponding frequency regions via ABRs (Figure 3, I–K). This result indicates that differences in neuronal origin (e.g., reduction in synaptic ribbons) exert additional effects on the ABR responses.

In agreement with the hearing test results, control mice showed significant hair cell loss at the age of 17 months; most of the OHCs were absent (Figure 4A), whereas only minor loss of OHCs was observed in the *Raptor-cKO* mice (Figure 4B). Quantification confirmed a greater retention of hair cell numbers in *Raptor-cKO* mice (Figure 4G). Thus, inactivation of mTORC1 signaling promoted hair cell survival in the aging inner ear. Furthermore, we investigated whether the number of synaptic ribbons, which were immunostained with antibodies against CtBP2/Ribeye, was different between aged controls and *Raptor-cKO* mice. Although most IHCs remained intact in control mice, numbers of synaptic ribbons in the remaining IHCs were strikingly reduced compared with those in *Raptor-cKO* mice (Figure 4, C–F and H), supporting the involvement of synapses rather than cell bodies in the deterioration of hearing in aged control mice. Damage of sensory hair cells in the organ of Corti is frequently associated with the secondary degeneration of SGNs. Thus, we counted SGNs in the middle region; nevertheless, no significant difference was found between *Raptor-cKO* and control mice (Figure 4, I and J). Taken together, these results provide evidence that inactivation of mTORC1 signaling in NSE alleviates ARHL.

Sustained mTORC1 activation has no effect on the initial maturation of hearing. Since mTORC1 activity is significantly increased in aged cochlea, and inactivation of mTORC1 signaling in NSE alleviates ARHL, we used a genetic approach to increase mTORC1 signaling selectively in NSE to further determine the mechanism through which NSE mTORC1 activity promotes ARHL. mTORC1 is under tonic inhibition by the Tsc1/Tsc2 complex, and *Tsc1* deletion results in constitutively increased mTORC1 signaling (33).

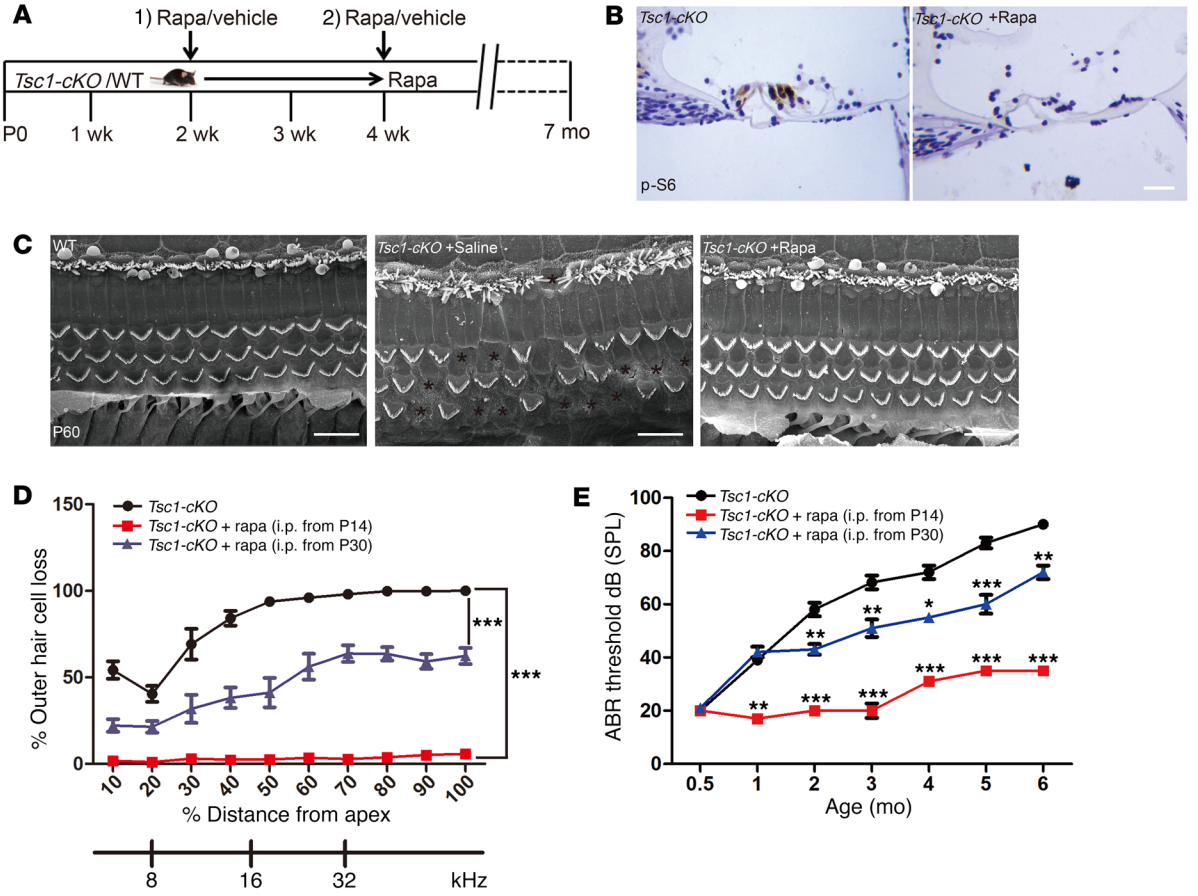

Figure 8. Rapamycin treatment prevents the hearing loss phenotype in *Tsc1-cKO* mice. (**A**) Schematic of rapamycin treatment (1 mg/kg i.p. every other day) to examine its effects on hearing in *Tsc1-cKO* mice. (**B**) Immunohistochemistry to detect p-S6 and hematoxylin staining of cochlear sections from *Tsc1-cKO* mice treated with or without rapamycin. $n = 3$. Scale bar: 20 μm. (**C**) SEM images showed that many hair cells disappeared in the middle turn of the cochlea in *Tsc1-cKO* mice; however, there were no obvious differences between *Tsc1-cKO* mice injected with rapamycin and WT control mice. $n = 3$. Scale bars: 10 μm. (**D**) Cochleograms of *Tsc1-cKO* mice ($n = 8$), *Tsc1-cKO* mice treated with rapamycin starting at P14 ($n = 10$), and *Tsc1-cKO* mice treated with rapamycin starting at P30 ($n = 10$). The cochleograms were recorded in the mice at 5 months of age. Graph shows the percentage loss of OHCs as a function of percentage distance from the apex. (**E**) Age-related click ABR hearing threshold results for *Tsc1-cKO* mice ($n = 8$), *Tsc1-cKO* mice treated with rapamycin starting at P14 ($n = 10$), and *Tsc1-cKO* mice treated with rapamycin starting at P30 ($n = 10$) at the same time points. Data represent the mean ± SEM. $^*P < 0.05$, $^{**}P < 0.01$, $^{***}P < 0.001$, by 2-tailed Student's *t* test or 1-way ANOVA with Holm-Šidák multiple-comparisons test.

We crossed $Tsc1^{fl/fl}$ mice with *Atoh1-Cre*–transgenic mice to produce *Tsc1-cKO* mice (Figure 5A). *Tsc1-cKO* mice were born with normal Mendelian ratios and grew normally. Western blot analysis of Tsc1, Tsc2, and p-S6 (235/236) expression showed that the Tsc1/Tsc2 complex is functionally disrupted, and mTORC1 activity increased in *Tsc1-cKO* mice (Figure 5B). In contrast, activation of mTORC1 signaling did not appear to affect the function of mTORC2, as the expression levels of p-Akt (Ser473) were unchanged in the NSE of *Tsc1-cKO* mice (Figure 5B). Thus, *Tsc1-cKO* mice demonstrate NSE-specific ablation of the *Tsc1* gene accompanied by overactivation of mTORC1 signaling without alterations in mTORC2 activity.

No significant differences were observed in hearing between age-matched WT and *Tsc1-cKO* mice at 2 weeks of age (Figure 5C), when hearing threshold can be tested in mice. No obvious changes in gross tissue morphology were detected in either the cochlea or the vestibule (data not shown). Whole-mount staining of the dissected sensory epithelia of *Tsc1-cKO* mice with the hair cell–specific marker Myo7A and phalloidin revealed no obvious structural abnormalities at 2 weeks of age, suggesting that the development of IHCs and OHCs in *Tsc1-cKO* was normal (Figure 5D). For higher-resolution studies, scanning electron microscopy (SEM) was performed to characterize cochlear hair cell stereocilia; according to the results, the bundles of OHCs in *Tsc1-cKO* mice appeared similar in size to those in controls and formed a normal staircase pattern at 2 weeks of age (Figure 5E). Additionally, we used the fluorescent dye FM1-43 to examine the functional mechanotransduction of cochlear hair cells. FM1-43 labeling in *Tsc1-cKO* hair cells was indistinguishable from that in controls at postnatal day 8 (P8), suggesting that the early development and function of hair cells was not affected in *Tsc1-cKO* mice (Figure 5F). In addition, cochleae of *Tsc1-cKO* mice did not show any changes in the expression levels or localization of markers for differentiating hair cells (prestin), supporting cells (Sox2), and neurons (neurofilament) (Figure 5F). Although Atoh1 also functions in vestibular hair cells, the shapes of the kinocilia and stereocilia in the vestibule were normal in *Tsc1-cKO* mice (data not shown). Together, these data demonstrated that sustained mTORC1 acti-

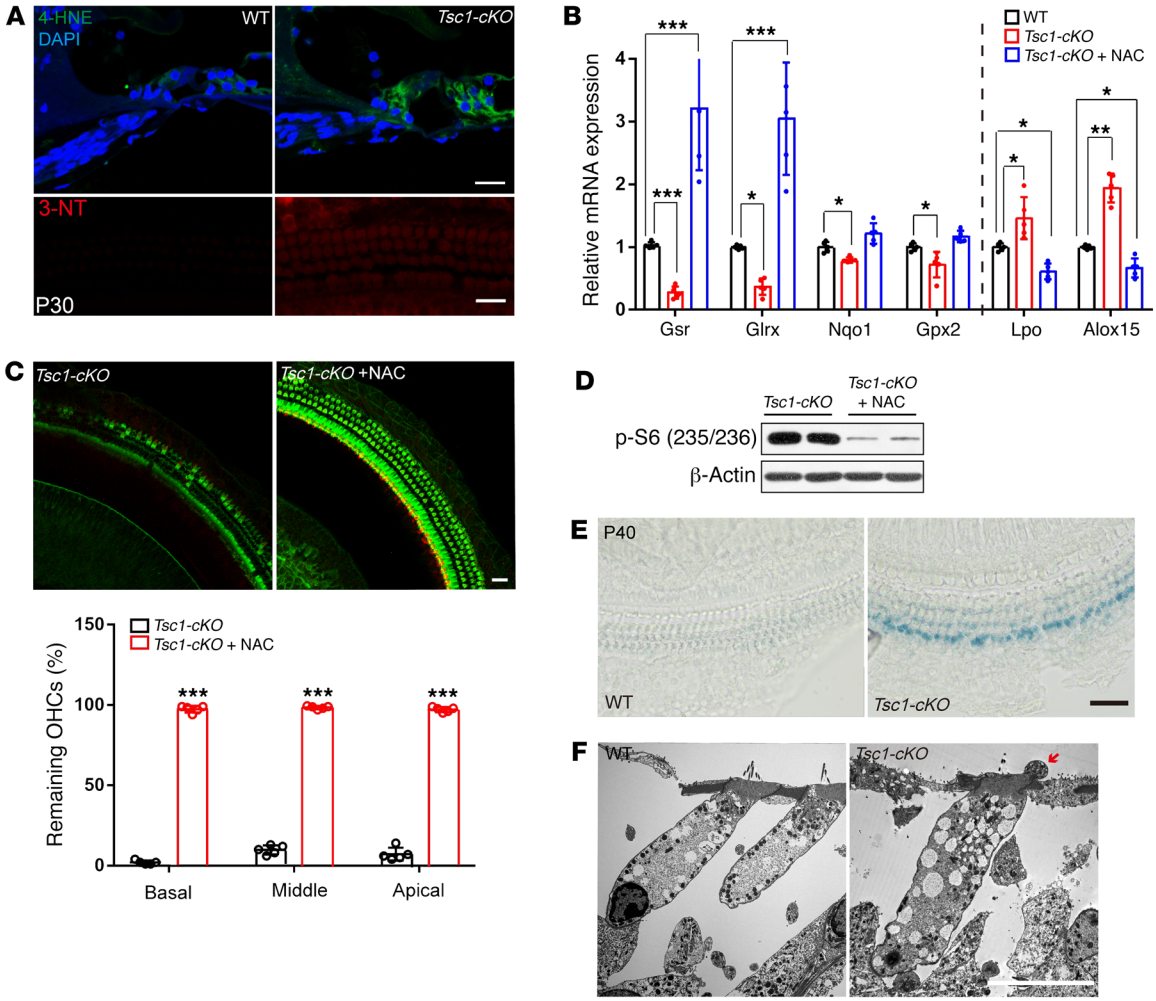

Figure 9. *Tsc1-cKO* mice exhibit oxidative stress in the organ of Corti. (**A**) Immunolabeled 4-HNE (green) and 3-NT (red) staining in the organ of Corti with DAPI staining (blue) in *Tsc1-cKO* mice was stronger than that in WT controls at P30. $n = 3$. Scale bars: 20 μm. (**B**) Quantitative real-time PCR analysis of collected inner hair cells showed that the expression levels of the antioxidant factors *Gsr*, *Glrx*, *Nqo1*, and *Gpx2* were significantly decreased, while the levels of the pro-oxidant factors *Lpo* and *Alox15* were significantly increased, in *Tsc1-cKO* mice compared with WT controls; however, the expression levels of the antioxidant factors *Gsr* and *Glrx* were significantly increased, and the levels of the pro-oxidant factors *Lpo* and *Alox15* were significantly increased, in *Tsc1-cKO* mice ($n = 5$) injected with rapamycin compared with WT controls ($n = 5$). (**C**) Effects of NAC on hair cell survival in *Tsc1-cKO* mice ($n = 5$). Scale bar: 20 μm. (**D**) Effects of NAC on mTORC1 signaling activity. Western blot analysis results are presented as the relative expression in *Tsc1-cKO* mice with or without NAC treatment ($n = 4$). (**E**) Representative senescence-associated β-galactosidase (SA β-gal) staining of the basilar membrane of the cochlea in *Tsc1-cKO* ($n = 3$) and WT mice ($n = 3$) at P40. Scale bar: 20 μm. (**F**) TEM images of normally appearing OHCs in WT mice and abnormal morphology of OHCs ($n = 5$) in *Tsc1-cKO* mice. The cytoplasm of OHCs shows numerous abnormal vacuoles. The cell bodies also show several aberrant structures (red arrow) in *Tsc1-cKO* mice. Scale bar: 10 μm. Data represent the mean ± SEM. $^*P < 0.5$, $^{**}P < 0.01$, $^{***}P < 0.001$, by 2-tailed Student's *t* test.

vation is not essential for the initial patterning of the cochlear NSE or the early development of hearing.

Sustained mTORC1 activation in NSE causes accelerated hearing loss at later ages. We continued to analyze the effects of mTORC1 activation on the NSE in *Tsc1-cKO* mice over time. Loss of OHCs in the basal turn was occasionally detected in *Tsc1-cKO* cochleae at 4 weeks of age, with no apparent changes in IHCs at the same age. Hair cell loss increased with age; by 4 months of age, no OHCs and very few IHCs remained in the middle and basal turns of the cochleae (Figure 6, A–L). We then examined hearing ability in *Tsc1-cKO* mice by measuring the ABR thresholds. At 2 weeks of age, the ABR thresholds were 20 ± 5 dB sound pressure level (SPL) in both *Tsc1-cKO* and control mice, but this increased rapidly in *Tsc1-cKO* mice, reaching 65 ± 5 dB SPL by the age of 8 weeks (Figure 6M). These results indicated the rapid loss of hearing in *Tsc1-cKO* mice. We also recorded DPOAEs to explore the functions of the cochlear outer cells (OHCs) in *Tsc1-cKO* and control mice. At P14, the *Tsc1-cKO* and control mice generated similar DPOAEs. With age, the DPOAEs of *Tsc1-cKO* mice were attenuated faster compared with those of the controls (Figure 6N). This degenerative pattern was also confirmed by SEM results for the epithelia in *Tsc1-cKO* and WT mice. There were no abnormalities in the structure of hair cells in *Tsc1-cKO* mice compared with that in control mice at P14. However, by P40, OHCs were partially degenerated, while all IHCs were still present along the cochlea (Figure 7B). Finally, by 4 months, most OHCs were lost throughout the entire cochlear epithelium in *Tsc1-cKO* mice (Figure

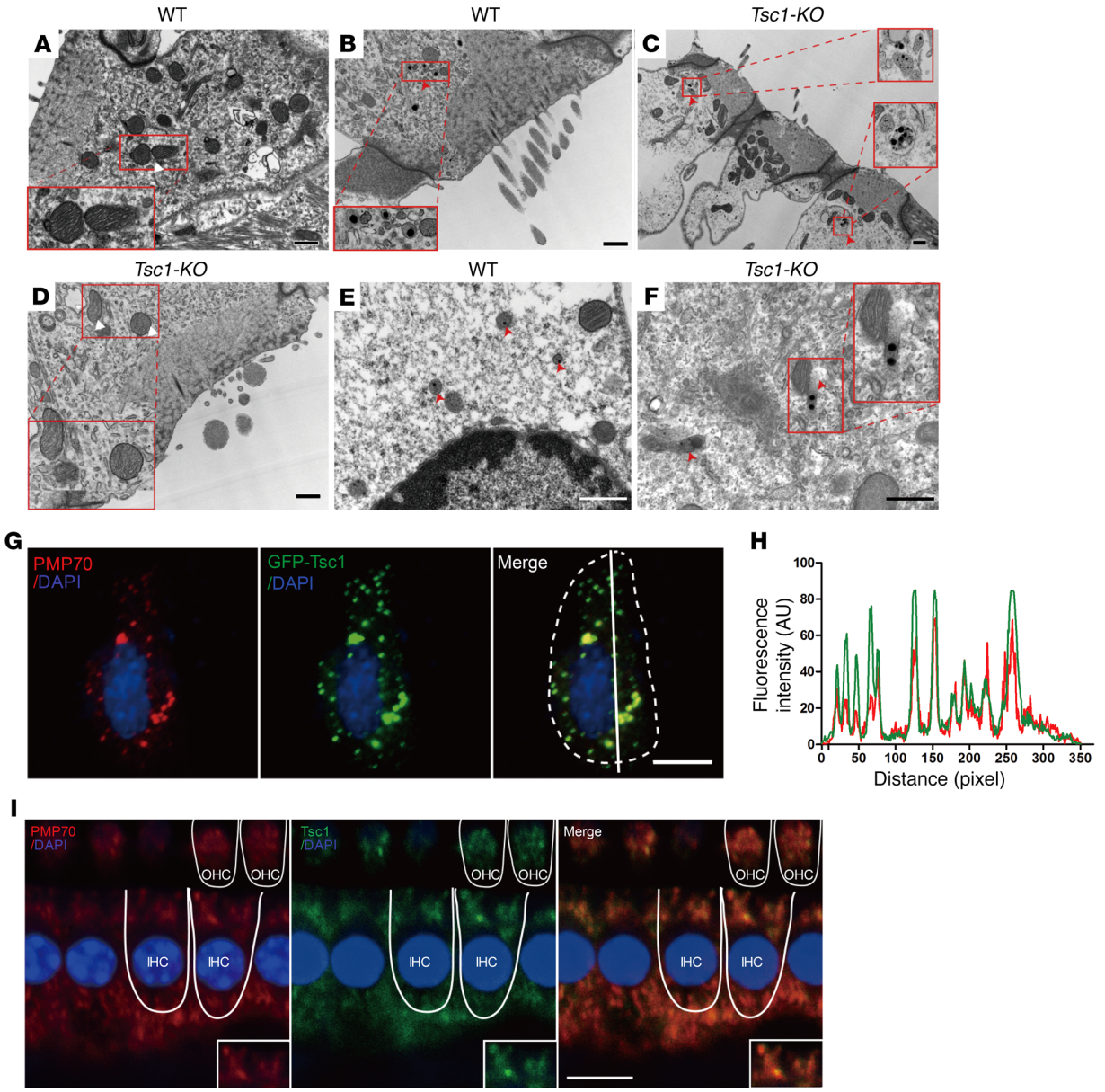

Figure 10. Peroxisomes are involved in the regulation of mTORC1 in inner ear hair cells. (**A**–**F**) TEM analysis revealing the morphologies of mitochondria and peroxisomes in cochlear OHCs of WT and *Tsc1-cKO* mice at P28. (**A** and **D**) No mitochondrial abnormalities were seen at this time point in *Tsc1-cKO* mice compared with WT controls. The mitochondria showed normal morphologies with defined lamellar cristae. (**B**, **C**, **E**, **F**) Normally, peroxisomes (red arrowheads) demonstrate a circular cytoplasmic arrangement around a central nucleus in WT mice (**B** and **E**). However, many crystalline nuclei appeared in the peroxisomes of *Tsc1-cKO* OHCs (**C**), and several abnormal peroxisomes had no evident membrane structures (**F**). Scale bars: 1 μm (**A**–**C**), 0.5 μm (**D**–**F**). (**G**) Tsc1 is associated with peroxisomes in transfected HEI-OC1 cells. Transfected HEI-OC1 cells producing Tsc1 (Tsc1-GFP, green) were coimmunostained with an antibody against PMP70 (red). Cell nuclei were stained with DAPI (blue). Scale bar: 10 μm. (**H**) Corresponding line intensity measurements for each protein indicate strong colocalization of GFP (green) and PMP70 in peroxisomes. The fluorescence intensity was quantified using ImageJ (NIH). (**I**) Double immunolabeling of hair cells (IHCs and OHCs) for PMP70 (red) and endogenous Tsc1 (green). Scale bar: 10 μm. Three mice were examined for each genotype.

7C), whereas no abnormalities were observed in the structure of hair cells in WT mice (Figure 7, A and D). Lost IHCs and long fused IHC stereocilia were also occasionally observed (Figure 7, E–J). Hair cell degeneration was followed by progressive degeneration of the SGNs after 4 months in *Tsc1-cKO* mice (Supplemental Figure 3), leading to collapse of the organ of Corti. Taken together, these data provide compelling evidence that sustained mTORC1 overactivation in cochlear NSE affects the long-term survival of hair cells, subsequently causing early-onset progressive hearing loss.

Several molecules affect mTORC1 activity by regulating the Tsc1/Tsc2 complex. For example, *Pten* loss causes the activation of Akt, which in turn activates mTORC1 signaling by inhibiting the Tsc1/Tsc2 complex (31). However, *Pten* ablation in NSE in the same *Atoh1-Cre* mice did not cause hearing loss in mice (34). *Pten* knockout in hair cells was recently reported to prevent gentamicin-induced hair cell death (35). To explain this discrepancy, we determined the expression levels of downstream targets of *Pten* in *Pten-cKO* (*Pten* gene inactivated by *Atoh1-Cre*) cochleae. The

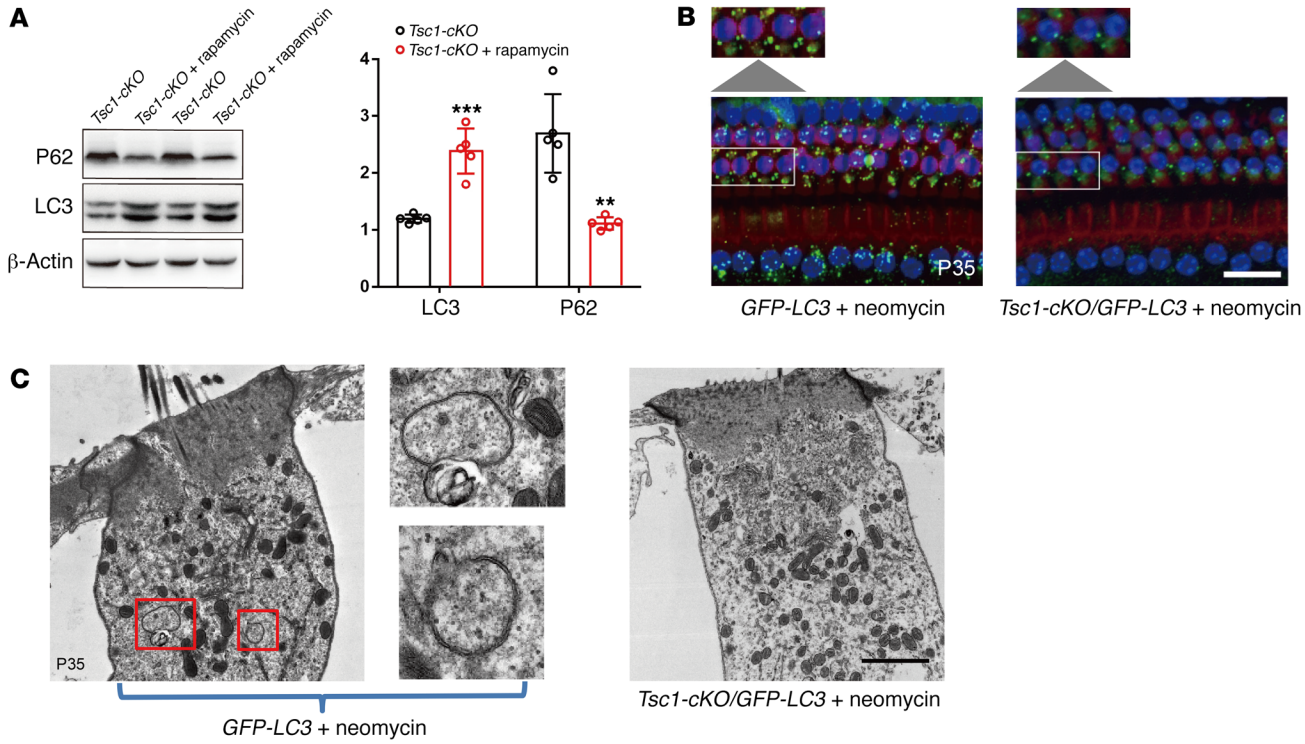

Figure 11. Autophagy in the auditory hair cells is disrupted in *Tsc1-cKO* mice. (**A**) Rapamycin enhanced autophagic flux in the cochleae of *Tsc1-cKO* mice. Western blotting analysis of LC3 and P62 expression in cochleae of untreated *Tsc1-cKO* mice and rapamycin-treated *Tsc1-cKO* mice. Densitometric analysis of the blots showing the ratios of LC3II and P62 to β-actin (n = 3). Values represent means ± SEM. (**B**) Representative images of *GFP-LC3* transgenic mice and *Tsc1-cKO/GFP-LC3* transgenic mice with neomycin treatment. Cytosolic GFP was diffuse and uniformly distributed throughout the cytoplasm in hair cells of *Tsc1-cKO/GFP-LC3* transgenic mice. In *GFP-LC3* transgenic mice, however, punctate GFP was observed. Enlarged images of OHCs outlined by white lines illustrate punctate fluorescence. Images were taken from the middle turn. n = 3. Scale bar: 2 μm. (**C**) Representative TEM images of autophagic vacuoles in outer hair cells of *GFP-LC3* transgenic mice and *Tsc1-cKO/GFP-LC3* transgenic mice with neomycin treatment. Enlarged images of OHCs outlined by the red lines indicate autophagic vacuoles in the outer hair cells. n = 3. Scale bar: 2 μm. Data represent the mean ± SEM. $^{**}P < 0.01$, $^{***}P < 0.001$, by 2-tailed Student's t test.

loss of *Pten*, unlike the loss of *Tsc1*, did not effectively promote mTORC1 activation (Supplemental Figure 4A), because p-S6 levels in *Pten-cKO* cochleae were lower than those in *Tsc1-cKO* mice. Thus, mTORC1 signaling levels in *Pten-cKO* cochleae may not be sufficient to damage hair cells. In contrast, p-Akt (S473) levels in *Pten-cKO* mice were higher than those in *Tsc1-cKO* mice (Supplemental Figure 4B). Akt regulates many downstream molecules in addition to the mTORC1 signaling pathway; thus, additional molecules downstream of activated Akt may attenuate mTORC1 activity and prevent the development of ARHL.

Rapamycin treatment prevents Tsc/mTORC1-dependent hearing injury and dysfunction. We hypothesized that if the abnormal activation of mTORC1 in *Tsc1-cKO* mice was directly responsible for inner hair cell loss, treatment with the mTORC1 inhibitor rapamycin should prevent progressive hearing dysfunction in these mice. To test this hypothesis, we started treating *Tsc1-cKO* mice with rapamycin at P14 and examined the effects for the next 5 months (Figure 8A). As expected, immunohistochemical staining of cochlear sections showed that elevated p-S6 levels were abolished in rapamycin-treated *Tsc1-cKO* mice at 3 months of age (Figure 8B). Mice treated with vehicle alone developed both hair cell loss and hearing defects, as expected, whereas none of the *Tsc1-cKO* mice treated with rapamycin showed similar symptoms at the same time points (Figure 8, C–E). These results demonstrated that rapamycin treatment starting from P14 protected the *Tsc1-cKO* mice from developing hearing loss later on and indicated that aberrant hyperactivation of mTORC1 signaling is required for accelerated hearing loss in *Tsc1-cKO* mice.

To determine whether hyperactivation of mTORC1 is also necessary for the process of deafness, we started rapamycin treatment at P30, the time point at which several symptoms of hearing defects begin to appear in *Tsc1-cKO* mice (Figure 8A). In contrast to the accelerated hearing loss in vehicle-treated mice, rapamycin treatment starting at P30 greatly slowed the process of hearing loss, as assessed by ABR measurements (Figure 8E). Consistent with the ABR results, hair cells of rapamycin-treated *Tsc1-cKO* mice also exhibited significantly increased survival rates compared with the controls when analyzed at 5 months of age (Figure 8D). In rapamycin-treated *Tsc1-cKO* mice at 7 months of age (i.e., rapamycin treatment for 6 months after starting at P30), only a small number of IHCs and OHCs exhibited traits associated with degeneration, and several SGCs showed traits of secondary degeneration; a large number of hair cells remained intact. In contrast, in vehicle-treated *Tsc1-cKO* mice, all outer hair cells died. Compared with rapamycin treatment starting at P14, rapamycin treatment starting at P30 failed to reverse the phenotypes of accel-

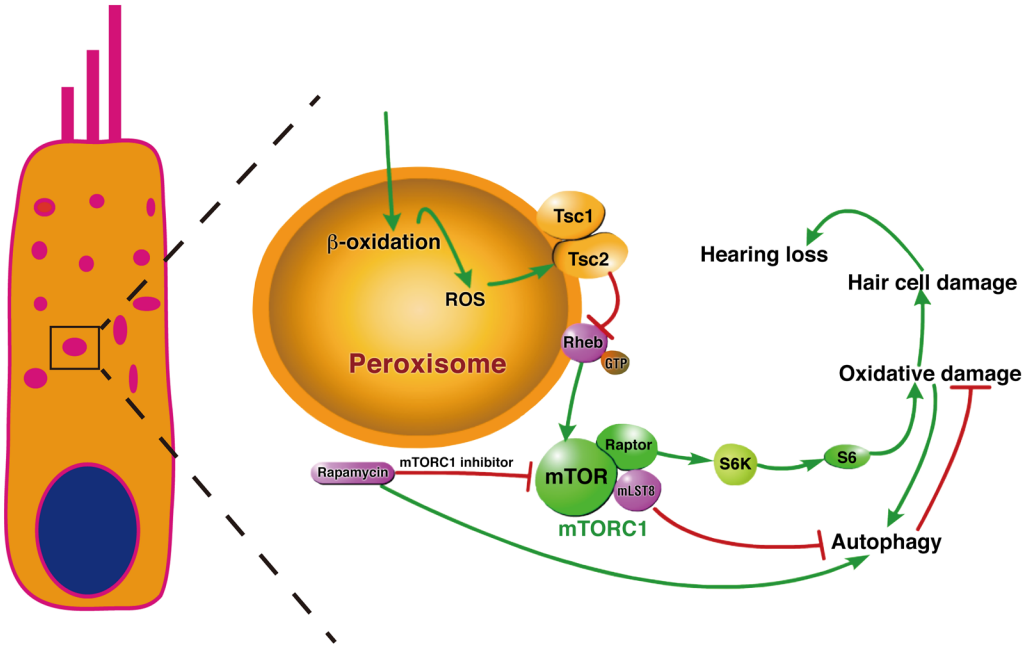

Figure 12. Overview of the regulation of redox homeostasis and Tsc/mTORC1 signaling in cochlear hair cells. In response to ROS, the Tsc complex localized to the peroxisome to regulate mTORC1 signaling and autophagy in hair cells. Deletion of *Tsc1* caused hyperactivation of mTORC1 signaling, inducing oxidative damage and autophagy breakdown, which further resulted in hair cell damage and caused hearing deficits. Conversely, deletion of the mTORC1 component *Raptor* inactivated mTORC1 signaling, thus promoting the survival of hair cells and delaying the process of ARHL in C57BL/6J mice. Injection of rapamycin, which is an mTORC1 inhibitor, also protected cells against oxidative stress, thus preventing the development of ARHL.

erated hearing loss in *Tsc1-cKO* mice, which suggested that once hearing damage occurred, the changes were unable to be rescued by rapamycin treatment. Based on these results, mTORC1-dependent pathological hearing phenotypes are prevented by the inhibition of mTORC1 with rapamycin prior to a certain time point.

ROS are involved in mTORC1-dependent hair cell damage in the cochleae of Tsc1-cKO mice. Having identified a pivotal role for the aberrant hyperactivation of mTORC1 signaling in progressive hearing loss, we sought to uncover the underlying downstream pathogenic mechanism. As an essential integrator of multiple intrinsic signals, mTORC1 signaling has been linked to many different downstream pathways, including protein synthesis, transcription, and oxidative stress (36). Among these pathways, we focused on oxidative stress, a well-characterized downstream target of mTORC1 signaling (37, 38). Previous studies have established that ROS play a substantial role in the aging process of cochlear cells. Thus, we hypothesized that the accumulation of oxidative damage to macromolecules followed by loss of their function is a primary underlying cause of premature hearing loss in *Tsc1-cKO* mice. The lipid peroxidation of ROS was assessed in P30 *Tsc1-cKO* mice by immunofluorescence-based detection of the ROS markers 4-hydroxynonenal (4-HNE) and 3-nitrotyrosine (3-NT). Immunolabeling of both 3-NT and 4-HNE increased dramatically in hair cells and supporting cells compared with controls (Figure 9A). Thus, hyperactivation of mTORC1 signaling resulted in ROS-induced cell damage in *Tsc1-cKO* mice. Cellular redox homeostasis depends on the pro-oxidant–antioxidant balance, and an increase in ROS levels might be caused by increased pro-oxidant levels and/or decreased antioxidant levels. We therefore examined the expression levels of genes involved in redox balance. Quantitative PCR results showed significantly decreased expression levels of several antioxidant enzymes (*Gpx2*, *Gsr*, *Nqo1*, and *Glrx*) and significantly increased expression levels of pro-oxidant enzymes (*Lpo*, *Alox15*) (Figure 9B), suggesting that *Tsc1-cKO* mice have impaired antioxidant defenses and exhibit features of marked oxidative stress in the cochleae. However, i.p. injection of rapamycin restored normal redox balance (Figure 9B). To further verify whether the increase in ROS levels contributed to the increased injury to *Tsc1-cKO* NSE, *N*-acetylcysteine (NAC), a common antioxidant, was used to treat *Tsc1-cKO* mice starting at P14. Following 2 months of NAC treatment in vivo, hair cell loss was dramatically abrogated in NAC diet–fed *Tsc1-cKO* mice, with no significant differences in body weight observed between NAC diet–fed groups and controls (Figure 9C). Remarkably, NAC treatment decreased the expression of p-S6 (235/236) in the sensory epithelia of *Tsc1-cKO* mice (Figure 9D). All these results demonstrate that increased ROS are likely the major underlying cause of the severe injury to the auditory NSE in *Tsc1-cKO* mice. Moreover, oxidative stress reportedly contributes to premature senescence in auditory cells (39). NAC also inhibits mTORC1, which in turn prevents senescence. Thus, we wondered whether the early onset of hair cell loss in *Tsc1-cKO* was caused by premature senescence. Whole mounts stained with senescence-associated β-galactosidase (SA β-gal; a widely known biomarker of cellular senescence) were analyzed in P42 *Tsc1-cKO* and control mice. Light microscopic analysis showed that nearly all hair cells are SA β-gal–positive in *Tsc1-cKO* mice (Figure 9E), and hair cells exhibited marked morphological changes, including changes in organelles and intracytoplasmic vacuoles (Figure 9F), which corresponded to characteristics of senescent cells.

Structural abnormalities of peroxisomes in hair cells exposed to sustained mTORC1 activation after P30. Impaired mitochondrial and peroxisomal functions are linked to disequilibrium of the antioxidant–pro-oxidant balance. To further uncover the mechanisms underlying oxidative stress in *Tsc1-cKO* mice, we examined the ultrastructural morphology of the mitochondria and peroxisomes in inner ear hair cells. Auditory hair cells possess many mitochondria and consume large amounts of oxygen and thus are sensitive to oxidative stress. However, we observed no evidence to suggest that mitochondria are damaged in *Tsc1-cKO* OHCs at P28 based

on transmission electron microscopy (TEM) analysis (Figure 10, A and D), and pathological changes to the mitochondria were not observed until P50, suggesting that the initial elevation of ROS is not attributable to mitochondrial defects. This finding is particularly intriguing in light of the fact that mitochondrial defects are a common cause of ROS overproduction. Peroxisome dysfunction may also cause ROS accumulation associated with hearing loss. Peroxisomes are extraordinarily dynamic ER-derived organelles that interact with other subcellular compartments to regulate major cellular functions related to the redox status of the cell. Recent reports have brought peroxisomes to the forefront of noise-induced hearing loss research (40, 41). Based on these reports, we investigated the morphology of peroxisomes by TEM. The shapes of peroxisomes in OHCs differed between *Tsc1-cKO* and WT mice at P30; many peroxisomes contained 3 to 5 crystal nuclei, and several abnormal peroxisomes did not even possess a distinct membrane structure (Figure 10, B, C, E, F). Thus, in the inner ear hair cells, peroxisomes, rather than mitochondria, are likely the primary organelles attacked by activated mTORC1 signaling.

The peroxisome is the central signaling organelle involved in the regulation of mTORC1 in inner ear hair cells. We next investigated the mechanism underlying how mTORC1 activation induces peroxisomal dysfunction in inner ear hair cells. Subcellular localization has emerged as an important determinant of mTORC1 function (42, 43). The TSC signaling node was recently shown to localize to peroxisomes, where it regulates mTORC1 in response to ROS in the FAO cell line (42). Therefore, we transiently transfected HEI-OC1 cells with a mouse mTsc1-GFP fusion construct in which the mouse *Tsc1* coding sequence was fused in-frame to the N-terminus of GFP. *mTsc1-GFP* was colocalized with peroxisomal membrane protein 70 (PMP70), a marker of peroxisomal membranes, in transfected HEI-OC1 cells (Figure 10G). Colocalization of mTsc1-GFP and peroxisomes was confirmed by measurement of the fluorescent intensities of GFP and PMP70 staining (Figure 10H). We also transfected a mutant version of mTsc1-GFP that lacks a PTS1 sequence (the targeting signal for the import of peroxisomal matrix proteins into the organelle), termed mTsc1$^{(-PTS1)}$-GFP, and found that the mutant mTsc1-GFP did not localize to the peroxisome but rather dispersed in the cytoplasm of HEI-OC1 cells (Supplemental Figure 5). Peroxisome localization of Tsc1 was also observed in COS7 cells, confirming the generalizability of its localization in other cell types (data not shown). In inner ear hair cells, Tsc1 colocalized with PMP70 according to immunolocalization studies of endogenous proteins (Figure 10I). Subcellular fractionation of auditory cells confirmed that the central node of mTORC1 signaling (endogenous Tsc1, Tsc2, and Rheb) is localized in the peroxisome fraction, and negligible amounts were found in other organelles (Supplemental Figure 6). Drugs such as fibrates (for example, Wy-14643) activate peroxisome proliferator–activated receptor-α (PPARα), to increase levels of peroxisomal ROS (44). The organ of Corti was treated with Wy-14643 and exhibited suppressed mTORC1, indicating that peroxisome ROS can directly stimulate auditory cells to reduce mTORC1 (Supplemental Figure 7). Thus, these results indicated that the peroxisome serves as the central signaling organelle involved in the regulation of mTORC1 in inner ear hair cells.

Autophagic activity is disrupted in the cochlear hair cells of Tsc1-cKO mice. According to numerous biochemical and genetic studies, mTORC1 negatively regulates autophagy. Recent studies have also revealed that autophagy plays essential roles in the mouse inner ear, and autophagy attenuates noise-induced hearing loss by reducing oxidative stress (45). As rapamycin is an effective autophagy activator and protects *Tsc1-cKO* cochlear hair cells from injury, we wondered whether autophagic activity was affected in the cochleae of *Tsc1-cKO* mice. Modification of microtubule-associated protein 1 light chain 3 (LC3) expression levels, specifically the shift from LC3I to LC3II expression, is one of the initiating steps in autophagosome formation. Our results showed that rapamycin injection induced the upregulation of LC3II in *Tsc1-cKO* mouse cochleae (Figure 11A). Our data also revealed decreased levels of P62/SQSTM1, a specific substrate that binds to LC3 to facilitate the degradation of ubiquitinated proteins (Figure 11A). Therefore, we speculated that autophagic flux dysfunction is one cause of the early-onset degeneration of hair cells in *Tsc1-cKO* mice. Recent reports have shown that aminoglycoside antibiotics induce autophagy when injected i.p. in rats (46). However, the basal levels of autophagy were very low in the cochleae, since little LC3II was detected. To increase the sensitivity of detection, we injected neomycin (an aminoglycoside antibiotic) into *Tsc1-cKO*/GFP-LC3 mice and control mice once per day for 5 consecutive days starting at P30 to increase autophagic flux. The autophagic response in auditory hair cells within the organ of Corti was then analyzed using immunofluorescence. Immunofluorescence analysis of the organ of Corti revealed that punctuate GFP fluorescence in OHCs in GFP-LC3 mice was much higher than that in *Tsc1-cKO*/GFP-LC3 mice (Figure 11B). Additionally, we used TEM to examine ultrastructural autophagic processes in auditory hair cells within the organ of Corti, and our data revealed that several autophagosomes (round, double-membraned structures) appeared 5 days after neomycin injection in GFP-LC3 mice, whereas no autophagosomes were observed in *Tsc1-cKO*/GFP-LC3 mice (Figure 11C). Together, these observations indicate that autophagy is dysregulated in *Tsc1-cKO* mice.

Discussion

A great deal of evidence has demonstrated that mTORC1 signaling plays a key role in the aging process of diverse organisms, and reduced mTORC1 signaling via genetic manipulation or inhibition of mTORC1 signaling with rapamycin treatment delays the onset of age-related disease and extends lifespan in vivo. However, whether mTORC1 signaling is involved in the development of ARHL is unknown.

In the present study, we found that immunofluorescent staining of p-S6 (235/236), a marker of mTORC1 activity, increased in cochlear hair cells but not in the spiral ganglion or stria vascularis in aged C57BL/6J mice. It is unclear why p-S6 (235/236) specifically increased in the cochlear NSE, and mTORC1 signaling may have different functions depending on the cell type. Total p-S6 levels in aged mice also showed enhanced detection by Western blot using cochlear sensory epithelia, possibly because hair cells and supporting cells may dominate the populations of cells responding to p-S6. However, further studies are required to uncover how mTORC1 signaling is regulated in different parts of the cochleae in aged mice. Moreover, Tsc1 levels were reduced in aged C57BL/6J mice, which may account for the enhanced mTORC1 activity. To confirm whether changes in mTORC1 activity affected the survival

of cochlear hair cells, we first determined that treatment with rapamycin, an inhibitor of mTORC1 signaling, prevented ARHL, indicating that mTORC1 signaling is involved in the development of ARHL. However, prolonged rapamycin treatment has been reported to promote Akt activation (47–49), which may also participate in the prevention of ARHL. To exclude this possibility, we generated mouse models in which the *Raptor* gene was specifically deleted in the cochlear NSE. Using p-S6 (235/236) as a marker of mTORC1 activity, we demonstrated that mTORC1 activity was greatly decreased after *Raptor* deletion. Genetic reduction of mTORC1 activity in the cochlear NSE alleviated ARHL in *Raptor-cKO* mice. Furthermore, we also generated mouse models in which the *Tsc1* gene was specifically deleted in the cochlear NSE. Although the *Tsc1-cKO* mice lost hair cells much faster than controls, rapamycin treatment prevented hearing loss if it was initiated by P14, which is consistent with the effects of rapamycin on ARHL, indicating that *Tsc1-cKO* mice share several features of ARHL with aged mice. Thus, our data suggest that Tsc/mTORC1 signaling activity may be a critical factor in the development of ARHL.

ARHL is characterized by an age-dependent decline in auditory function associated with the loss of sensory hair cells, SGNs, and stria vascularis cells in the cochlea of the inner ear. Recently, oxidative stress, i.e., the imbalance between the production of ROS and the detoxification of reactive intermediates, has been shown to be involved in the pathogenesis of ARHL (10, 50–52). The excessive production of ROS overwhelms antioxidant defense systems and causes irreversible oxidative damage to DNA, proteins, and lipids within the cochlear cells. Additionally, antioxidant therapy has been attempted with some success in models of noise-induced hearing loss and ARHL (13, 53). Recently, ROS levels were reported to be affected by changes in mTORC1 signaling, indicating a link between redox balance and mTORC1 signaling (54–56). In the present study, levels of 3-NT and 4-HNE, which are markers of ROS, were increased in 1-month-old *Tsc1-cKO* cochleae, indicating high levels of oxidative stress. Additionally, the hearing defects in *Tsc1-cKO* mice were almost completely prevented by NAC treatment starting at P14. NAC is known to possess strong antioxidant properties and scavenges ROS. Recently, Ding et al. reported that hearing deficits and IHC loss were completely prevented by NAC treatment (12). However, the ability of NAC to prevent ARHL is controversial, because Davis et al. did not confirm the protective effects of NAC against ARHL in aged C57BL/6J mice (57). Future studies are required to determine whether the treatment initiation time, the duration, or the dosage of NAC treatment affects its preventive effects against ARHL.

Mitochondria are thought to be a major source of ROS production and play a key role in aging. ROS damage key mitochondrial components, including mitochondrial DNA and respiratory chain complex proteins. Such damage accumulates with time and ultimately leads to permanent age-related mitochondrial dysfunction; loss of mitochondrial integrity further leads to increased ROS production and the release of ROS into the cytoplasm, which in turn contributes to cellular aging phenotypes. Mitochondrial ROS production had been identified as a major source of oxidative stress in inner ear cells (10, 14). However, in the present study, Tsc1 localized to the peroxisomes in hair cells, and *Tsc1-cKO* peroxisomes displayed structural abnormalities much earlier than the mitochondria, accompanied by high levels of oxidative stress markers in the cochlea and gene expression changes consistent with redox imbalance. Peroxisomes are highly dynamic organelles involved in several key cellular functions related to the metabolic and redox status of the cell, including bile acid synthesis, glyoxylate and dicarboxylate metabolism, D-amino acid metabolism, and β-oxidation of branched and very-long-chain fatty acids. Importantly, D-amino acid metabolism and peroxisomal β-oxidation result in the production of ROS and reactive nitrogen species, which, in excess, cause cellular damage and trigger catabolic functions such as autophagy. Recently, the TSC signaling node (Tsc1, Tsc2, and Rheb) was reported to localize to the peroxisome (58). When TSC signaling was activated by peroxisomal ROS, repression of mTORC1 occurred, which increased autophagic flux in the cell. In the present study, autophagy was disturbed in *Tsc1-cKO* cochlear hair cells in which mTORC1 signaling was overactivated. We also demonstrated that inhibition of mTORC1 signaling with rapamycin treatment increased the levels of LC3II, an autophagic marker that accumulates when autophagy is activated. Thus, these results suggest that the peroxisome may also play a critical role in the auditory system, and its dysfunction in cochlear hair cells may cause excessive ROS production and the dysregulation of autophagy, which in turn leads to hair cell damage. Future studies will be required to clarify the functions of peroxisomes in hair cells and the involvement of peroxisomal damage in hearing loss.

The mTORC1 inhibitor rapamycin has been shown to extend lifespan and mitigate disease. Here, we are the first, to our knowledge, to report that rapamycin treatment protects mice against ARHL. In the past several years, Fang and Xiao showed that rapamycin alleviates cisplatin-induced ototoxicity in vivo (59). Yuan et al. reported that rapamycin attenuates noise-induced hearing loss by reducing oxidative stress (45). Ebnoether et al. found that rapamycin protects sensory hair cells against gentamicin-induced damage (60). These data suggest that rapamycin may be a potential therapeutic drug for hearing loss. However, a key question regarding rapamycin use is its side effects, such as immunosuppression. Fortunately, several new rapamycin analogs, such as ATP-competitive mTOR inhibitors, have demonstrated surprisingly reduced side effects in lymphocytes compared with rapamycin, suggesting that these new drugs may be safer and less immunosuppressive. Thus, the ability of these analogs to prevent hearing loss should be tested.

In summary, our study demonstrates that increased mTORC1 activation is an important factor contributing to ARHL in aged mice, which exhibit disrupted redox balance and autophagy via peroxisomal perturbations (Figure 12). Dietary rapamycin treatment reduces cochlear hair cell loss. Our findings suggest that treatment with rapamycin or other "rapalogs" holds significant potential for the treatment of ARHL. Future studies should distinguish the role of peroxisomes from that of mitochondria in ARHL and evaluate the impact of mTORC1 activity on redox balance and autophagy.

Methods

Animal models. All animal experiments were approved by the Animal Ethics Committee of the School of Life Science, Shandong University. Animal management was performed strictly in accordance with the standards of the Animal Ethics Committee of the School of Life Science, Shandong University.

Male and female C57BL/6J mice were obtained from Beijing Vital River Laboratory Animal Technology Co. Ltd. *Rosa26-tdTomato* (no. 007914), *Pten*$^{fl/fl}$ (no. 004597), *Tsc1*$^{fl/fl}$ (no. 005680), and *Raptor*$^{fl/fl}$ (no. 013188) mice were obtained from The Jackson Laboratory. *Atoh1-Cre* mice were gifts from Lin Gan (University of Rochester, New York, New York, USA) (32). *GFP-LC3* mice (61) were obtained from RIKEN. The *Pten*$^{fl/fl}$, *Tsc1*$^{fl/fl}$, *Raptor*$^{fl/fl}$, and *Atoh1-Cre* mouse lines were backcrossed with the C57BL/6J line for 5 generations. We generated *Tsc1*$^{fl/fl}$ *Atoh1-Cre* (*Tsc1-cKO*), *Pten*$^{fl/fl}$ *Atoh1-Cre* (*Pten-cKO*), and *Raptor*$^{fl/fl}$ *Atoh1-Cre* (*Raptor-cKO*) mice, which were confirmed by PCR genotyping, and then sequenced the *Cdh23* gene from DNA obtained from the tails of young mice. Mice of either sex were used in all experiments. PCR genotyping primer sequences are listed in Supplemental Table 1.

In vivo auditory tests. Auditory brainstem responses (ABRs) and distortion product otoacoustic emissions (DPOAEs) were measured as described previously (ref. 62; and see Supplemental Methods).

Cell culture. A murine auditory cell line (HEI-OC1) was cultured in DMEM containing 10% heat-inactivated FCS (GIBGO-BRL) at 33°C under 5% CO_2. The COS7 cell line was cultured in DMEM containing 10% heat-inactivated FCS (GIBGO-BRL) at 37°C under 10% CO_2. Cells were transfected with pEGFP-mTsc1 using Lipofectamine 2000 (Invitrogen). The coding sequence of murine *Tsc1* was amplified by PCR and subcloned into the expression vector pEGFP-C2. Mouse *Tsc1* cDNA was obtained from the cochleae of C57BL/6J mice. *Tsc1* mutant constructs were generated via site-directed mutagenesis using a Stratagene QuikChange Kit (Agilent Technologies) and validated by DNA sequencing.

Histological analysis. Cochlea samples were fixed and decalcified using a procedure similar to that used for the immunostaining assay, dehydrated through an ethanol gradient series ranging from 30% to 100%, and embedded in paraffin. Sections were deparaffinized in xylene, rehydrated through an ethanol series, and stained with H&E. Sections were then dehydrated, coverslipped, and analyzed under a light microscope (Nikon YS100).

For SGN counting, immunolocalization studies, and electron microscopy analyses, see Supplemental Methods.

Rapamycin, ototoxic drug (neomycin), and oral antioxidant (NAC) treatment. Rapamycin (Sigma-Aldrich) was dissolved in 100% methanol at 20 mg/ml for storage at –20°C. A working solution was prepared in 0.25% Tween-80 and 0.25% polyethylene glycol 400 diluted in PBS. Postnatal treatment started at the 14th day after birth, and 1 mg/kg was administered i.p. every other day.

Neomycin at a dose of 120 mg/kg was administered i.p. for 5 consecutive days from P30. Then, cochleae were harvested for morphological evaluation.

A dose of 1% *N*-acetylcysteine (NAC; Sigma-Aldrich) was added to the drinking water of *Tsc1-cKO* mice during and after pregnancy. Therefore, the *Tsc1-cKO* pups (n = 6) received the drug in utero first, then via breast milk. *Tsc1-cKO* mice were continuously treated with NAC after weaning until P60. The drug dose was previously shown to be nontoxic. Possible side effects of NAC treatment were monitored throughout the study, and no differences were observed between the controls and *Tsc1-cKO* mice.

Isolation and collection of hair cells. Twenty *Atoh1-Cre/Tsc1/Rosa26-tdTomato* mice (P4) of either sex were used. The basilar membrane was isolated and transferred to a prewarmed digestion system (0.125% trypsin/EDTA). After digestion (37°C, 5 minutes), soybean trypsin inhibitor was added to terminate the reaction, followed by mechanical trituration with blunt tips and pipetting up and down 50–100 times. Suspended cells were percolated through a 40-μm cell strainer before FACS was performed. tdTomato-positive hair cells were sorted in a BD FACSAria III (BD Biosciences) using the tdTomato channel.

Single-cell isolation and cDNA synthesis. Single-cell isolation was performed as described previously (63). Apical and medial half-turns of the organ of Corti from 30-day-old WT and *Tsc1-cKO* mice were dissected and fixed on a coverslip. IHCs and OHCs were separately harvested with micropipettes (30 IHCs and 80 OHCs) under fast flow of a physiological solution (120 mM Na-gluconate, 35 mM NaCl, 4.8 mM KCl, 1.3 mM $CaCl_2$, 0.9 mM $MgCl_2$, 0.7 mM NaH_2PO_4, 10 mM HEPES, and 5.6 mM glucose; pH 7.35; 320 mOsm/kg) for preserving hair cells. Cells were immediately frozen in liquid nitrogen, and cDNA synthesis was performed with SuperScript III (Vazyme Biotech Co. Ltd.) following the manufacturer's instructions.

Quantitative real-time PCR. Quantitative real-time PCR was performed using the SYBR Premix Ex Taq reagent system (TakaRa) on a BioRad Sequence Detection System according to the manufacturer's instructions. Primer sequences are listed in Supplemental Table 2. Each reaction was performed in triplicate. The mRNA levels were calculated relative to the housekeeping gene β-actin and then analyzed using the $2^{-\Delta\Delta CT}$ method.

Extraction of proteins from formalin-fixed sensory epithelia and Western blot analysis. The extraction of proteins from formalin-fixed sensory epithelia was performed as described previously (ref. 64; and see Supplemental Methods).

Statistical analysis. Data are expressed as the mean ± SEM or SD as indicated from at least 3 independent experiments. Statistical analysis of the data was performed using a 2-tailed-distribution Student's t test or 1-way ANOVA followed by Bonferroni's multiple-comparison correction using GraphPad Prism 5.01 (GraphPad Software). For all tests, a P value less than 0.05 was considered statistically significant.

Study approval. Animal management was performed strictly in accordance with the standards of the Animal Ethics Committee of School of Life Science, Shandong University, which also approved all animal experiments.

Author contributions

JG and HW designed and supervised the project. XF, XS, LZ, YJ, RC, LY, and AZ performed experiments and acquired the data. XF, JG, HW, JL, XS, LZ, XL, and XB analyzed and interpreted the results. XF and JG wrote the manuscript.

Acknowledgments

We thank the laboratory of Weimin Tong for its help. This work was supported by grants from the Natural Science Foundation of China (no. 81670943) and the National 973 Basic Research Program of China (no. 2014CB541703).

Address correspondence to: Haibo Wang, Provincial Hospital Affiliated to Shandong University, Department of Otolaryngology — Head and Neck Surgery, Duanxing Xilu, Jinan 250117, Shandong, China. Phone: 86.531.68777588; Email: whbotologic797@163.com. Or to: Jiangang Gao, School of Life Science, Shandong University, 27 Shanda Nanlu, Jinan 250100, Shandong, China. Phone: 86.531.88365399; Email: jggao@sdu.edu.cn.

1. Ateş NA, et al. Glutathione S-transferase gene polymorphisms in presbycusis. *Otol Neurotol*. 2005;26(3):392–397.
2. Yamasoba T, Someya S, Yamada C, Weindruch R, Prolla TA, Tanokura M. Role of mitochondrial dysfunction and mitochondrial DNA mutations in age-related hearing loss. *Hear Res*. 2007;226(1–2):185–193.
3. Hu H, et al. The role of Efr3a in age-related hearing loss. *Neuroscience*. 2017;341:1–8.
4. Gopinath B, et al. Dietary antioxidant intake is associated with the prevalence but not incidence of age-related hearing loss. *J Nutr Health Aging*. 2011;15(10):896–900.
5. Huyghe JR, et al. Genome-wide SNP-based linkage scan identifies a locus on 8q24 for an age-related hearing impairment trait. *Am J Hum Genet*. 2008;83(3):401–407.
6. Yamasoba T. Interventions to prevent age-related hearing loss. In: Miller J, Le Prell C, Rybak L, eds. *Free radicals in ENT pathology. Oxidative stress in applied basic research and clinical practice*. Cha, Switzerland: Humana Press; 2015.
7. Sha SH, et al. Age-related auditory pathology in the CBA/J mouse. *Hear Res*. 2008;243(1–2):87–94.
8. Böttger EC, Schacht J. The mitochondrion: a perpetrator of acquired hearing loss. *Hear Res*. 2013;303:12–19.
9. Coling D, Chen S, Chi LH, Jamesdaniel S, Henderson D. Age-related changes in antioxidant enzymes related to hydrogen peroxide metabolism in rat inner ear. *Neurosci Lett*. 2009;464(1):22–25.
10. Jiang H, Talaska AE, Schacht J, Sha SH. Oxidative imbalance in the aging inner ear. *Neurobiol Aging*. 2007;28(10):1605–1612.
11. Le T, Keithley EM. Effects of antioxidants on the aging inner ear. *Hear Res*. 2007;226(1–2):194–202.
12. Ding D, et al. N-acetyl-cysteine prevents age-related hearing loss and the progressive loss of inner hair cells in γ-glutamyl transferase 1 deficient mice. *Aging* (Albany, NY). 2016;8(4):730–750.
13. Heman-Ackah SE, Juhn SK, Huang TC, Wiedmann TS. A combination antioxidant therapy prevents age-related hearing loss in C57BL/6 mice. *Otolaryngol Head Neck Surg*. 2010;143(3):429–434.
14. Someya S, et al. Age-related hearing loss in C57BL/6J mice is mediated by Bak-dependent mitochondrial apoptosis. *Proc Natl Acad Sci U S A*. 2009;106(46):19432–19437.
15. Deosaran E, et al. NBR1 acts as an autophagy receptor for peroxisomes. *J Cell Sci*. 2013;126(pt 4):939–952.
16. Shimobayashi M, Hall MN. Making new contacts: the mTOR network in metabolism and signalling crosstalk. *Nat Rev Mol Cell Biol*. 2014;15(3):155–162.
17. Laplante M, Sabatini DM. mTOR signaling in growth control and disease. *Cell*. 2012;149(2):274–293.
18. Bai X, Jiang Y. Key factors in mTOR regulation. *Cell Mol Life Sci*. 2010;67(2):239–253.
19. Gao X, et al. Tsc tumour suppressor proteins antagonize amino-acid-TOR signalling. *Nat Cell Biol*. 2002;4(9):699–704.
20. Johnson SC, Rabinovitch PS, Kaeberlein M. mTOR is a key modulator of ageing and age-related disease. *Nature*. 2013;493(7432):338–345.
21. Lamming DW, Sabatini DM. A central role for mTOR in lipid homeostasis. *Cell Metab*. 2013;18(4):465–469.
22. Yang J, et al. mTORC1 promotes aging-related venous thrombosis in mice via elevation of platelet volume and activation. *Blood*. 2016;128(5):615–624.
23. Neff F, et al. Rapamycin extends murine lifespan but has limited effects on aging. *J Clin Invest*. 2013;123(8):3272–3291.
24. Harrison DE, et al. Rapamycin fed late in life extends lifespan in genetically heterogeneous mice. *Nature*. 2009;460(7253):392–395.
25. Hine C, et al. Endogenous hydrogen sulfide production is essential for dietary restriction benefits. *Cell*. 2015;160(1–2):132–144.
26. Harputlugil E, Hine C, Vargas D, Robertson L, Manning BD, Mitchell JR. The TSC complex is required for the benefits of dietary protein restriction on stress resistance in vivo. *Cell Rep*. 2014;8(4):1160–1170.
27. Stanfel MN, Shamieh LS, Kaeberlein M, Kennedy BK. The TOR pathway comes of age. *Biochim Biophys Acta*. 2009;1790(10):1067–1074.
28. Colman RJ, et al. Caloric restriction delays disease onset and mortality in rhesus monkeys. *Science*. 2009;325(5937):201–204.
29. Someya S, Yamasoba T, Weindruch R, Prolla TA, Tanokura M. Caloric restriction suppresses apoptotic cell death in the mammalian cochlea and leads to prevention of presbycusis. *Neurobiol Aging*. 2007;28(10):1613–1622.
30. Zheng QY, Johnson KR, Erway LC. Assessment of hearing in 80 inbred strains of mice by ABR threshold analyses. *Hear Res*. 1999;130(1–2):94–107.
31. Zhou J, Brugarolas J, Parada LF. Loss of Tsc1, but not Pten, in renal tubular cells causes polycystic kidney disease by activating mTORC1. *Hum Mol Genet*. 2009;18(22):4428–4441.
32. Yang H, Xie X, Deng M, Chen X, Gan L. Generation and characterization of Atoh1-Cre knock-in mouse line. *Genesis*. 2010;48(6):407–413.
33. Adhikari D, et al. Tsc/mTORC1 signaling in oocytes governs the quiescence and activation of primordial follicles. *Hum Mol Genet*. 2010;19(3):397–410.
34. Kim HJ, et al. Conditional deletion of pten leads to defects in nerve innervation and neuronal survival in inner ear development. *PLoS One*. 2013;8(2):e55609.
35. Jadali A, Kwan KY. Activation of PI3K signaling prevents aminoglycoside-induced hair cell death in the murine cochlea. *Biol Open*. 2016;5(6):698–708.
36. Chen C, et al. TSC-mTOR maintains quiescence and function of hematopoietic stem cells by repressing mitochondrial biogenesis and reactive oxygen species. *J Exp Med*. 2008;205(10):2397–2408.
37. Wullschleger S, Loewith R, Hall MN. TOR signaling in growth and metabolism. *Cell*. 2006;124(3):471–484.
38. Cunningham JT, Rodgers JT, Arlow DH, Vazquez F, Mootha VK, Puigserver P. mTOR controls mitochondrial oxidative function through a YY1-PGC-1α transcriptional complex. *Nature*. 2007;450(7170):736–740.
39. Menardo J, et al. Oxidative stress, inflammation, and autophagic stress as the key mechanisms of premature age-related hearing loss in SAMP8 mouse Cochlea. *Antioxid Redox Signal*. 2012;16(3):263–274.
40. Delmaghani S, et al. Hypervulnerability to sound exposure through impaired adaptive proliferation of peroxisomes. *Cell*. 2015;163(4):894–906.
41. Mardones P, Hetz C. Peroxisomes get loud: a redox antidote to hearing loss. *Cell*. 2015;163(4):790–791.
42. Zhang J, et al. A tuberous sclerosis complex signalling node at the peroxisome regulates mTORC1 and autophagy in response to ROS. *Nat Cell Biol*. 2013;15(10):1186–1196.
43. Zhang J, et al. ATM functions at the peroxisome to induce pexophagy in response to ROS. *Nat Cell Biol*. 2015;17(10):1259–1269.
44. Zhang J, et al. A tuberous sclerosis complex signalling node at the peroxisome regulates mTORC1 and autophagy in response to ROS. *Nat Cell Biol*. 2013;15(10):1186–1196.
45. Yuan H, et al. Autophagy attenuates noise-induced hearing loss by reducing oxidative stress. *Antioxid Redox Signal*. 2015;22(15):1308–1324.
46. Kim YJ, et al. Autophagic flux, a possible mechanism for delayed gentamicin-induced ototoxicity. *Sci Rep*. 2017;7:41356.
47. Carracedo A, et al. Inhibition of mTORC1 leads to MAPK pathway activation through a PI3K-dependent feedback loop in human cancer. *J Clin Invest*. 2008;118(9):3065–3074.
48. Harston RK, et al. Rapamycin treatment augments both protein ubiquitination and Akt activation in pressure-overloaded rat myocardium. *Am J Physiol Heart Circ Physiol*. 2011;300(5):H1696–H1706.
49. Veilleux A, Houde VP, Bellmann K, Marette A. Chronic inhibition of the mTORC1/S6K1 pathway increases insulin-induced PI3K activity but inhibits Akt2 and glucose transport stimulation in 3T3-L1 adipocytes. *Mol Endocrinol*. 2010;24(4):766–778.
50. Fujimoto C, Yamasoba T. Oxidative stresses and mitochondrial dysfunction in age-related hearing loss. *Oxid Med Cell Longev*. 2014;2014:582849.
51. Menardo J, et al. Oxidative stress, inflammation, and autophagic stress as the key mechanisms of premature age-related hearing loss in SAMP8 mouse Cochlea. *Antioxid Redox Signal*. 2012;16(3):263–274.
52. Tadros SF, D'Souza M, Zhu X, Frisina RD. Gene expression changes for antioxidants pathways in the mouse cochlea: relations to age-related hearing deficits. *PLoS One*. 2014;9(2):e90279.
53. Fetoni AR, Picciotti PM, Paludetti G, Troiani D. Pathogenesis of presbycusis in animal models: a review. *Exp Gerontol*. 2011;46(6):413–425.
54. Dermit M, et al. Oxidative stress downstream of mTORC1 but not AKT causes a proliferative defect in cancer cells resistant to PI3K inhibition. *Oncogene*. 2017;36(19):2762–2774.
55. Luo Y, et al. Tsc1 expression by dendritic cells is required to preserve T-cell homeostasis and response. *Cell Death Dis*. 2017;8(1):e2553.
56. Nacarelli T, Azar A, Sell C. Mitochondrial stress induces cellular senescence in an mTORC1-dependent manner. *Free Radic Biol Med*. 2016;95:133–154.
57. Davis RR, Kuo MW, Stanton SG, Canlon B, Krieg

E, Alagramam KN. N-Acetyl L-cysteine does not protect against premature age-related hearing loss in C57BL/6J mice: a pilot study. *Hear Res*. 2007;226(1–2):203–208.
58. Zhang J, et al. A tuberous sclerosis complex signalling node at the peroxisome regulates mTORC1 and autophagy in response to ROS. *Nat Cell Biol*. 2013;15(10):1186–1196.
59. Fang B, Xiao H. Rapamycin alleviates cisplatin-induced ototoxicity in vivo. *Biochem Biophys Res Commun*. 2014;448(4):443–447.
60. Ebnoether E, Ramseier A, Cortada M, Bodmer D, Levano-Huaman S. Sesn2 gene ablation enhances susceptibility to gentamicin-induced hair cell death via modulation of AMPK/mTOR signaling. *Cell Death Discov*. 2017;3:17024.
61. Kuma A, Mizushima N. Chromosomal mapping of the GFP-LC3 transgene in GFP-LC3 mice. *Autophagy*. 2008;4(1):61–62.
62. Fu X, et al. Loss of Myh14 increases susceptibility to noise-induced hearing loss in CBA/CaJ mice. *Neural Plast*. 2016;2016:6720420.
63. Liu H, Pecka JL, Zhang Q, Soukup GA, Beisel KW, He DZ. Characterization of transcriptomes of cochlear inner and outer hair cells. *J Neurosci*. 2014;34(33):11085–11095.
64. Hill K, Yuan H, Wang X, Sha SH. Noise-induced loss of hair cells and cochlear synaptopathy are mediated by the activation of AMPK. *J Neurosci*. 2016;36(28):7497–7510.